

NASA TECHNICAL NOTE



NASA TN D-4396

C. 1



NASA TN D-4396

LOAN COPY: RETURN TO  
AFWL (WLIL-2)  
KIRTLAND AFB, N MEX

A PILOTED SIMULATOR STUDY  
OF TAKEOFF PERFORMANCE AND  
HANDLING QUALITIES OF A  
DOUBLE-DELTA SUPERSONIC TRANSPORT

*by C. Thomas Snyder and Charles T. Jackson, Jr.*

*Ames Research Center  
Moffett Field, Calif.*

NATIONAL AERONAUTICS AND SPACE ADMINISTRATION • WASHINGTON, D. C. • FEBRUARY 1968



A PILOTED SIMULATOR STUDY OF TAKEOFF PERFORMANCE  
AND HANDLING QUALITIES OF A DOUBLE-DELTA  
SUPERSONIC TRANSPORT

By C. Thomas Snyder and Charles T. Jackson, Jr.

Ames Research Center  
Moffett Field, Calif.

NATIONAL AERONAUTICS AND SPACE ADMINISTRATION

---

For sale by the Clearinghouse for Federal Scientific and Technical Information  
Springfield, Virginia 22151 - CFSTI price \$3.00

# TABLE OF CONTENTS

	<u>Page</u>
SUMMARY . . . . .	1
INTRODUCTION . . . . .	1
NOTATION . . . . .	2
TEST EQUIPMENT . . . . .	5
TEST CONFIGURATION . . . . .	8
TEST PROCEDURE . . . . .	11
RESULTS AND DISCUSSION OF BASIC TAKEOFF CHARACTERISTICS . . . . .	12
Ground Roll . . . . .	12
Rotation . . . . .	12
Effect of high pitch attitude on longitudinal acceleration . . . . .	12
Effect of high acceleration on $V_R$ and $V_{LOF}$ . . . . .	13
Rotation characteristics; ground clearance before lift-off . . . . .	14
Incompatibility with present airworthiness criteria . . . . .	16
Effects of abnormal rotations . . . . .	17
Transition . . . . .	19
Ground clearance after lift-off . . . . .	19
Transient characteristics leaving ground effect . . . . .	20
Effect of thrust setting on takeoff distance . . . . .	20
Takeoff time history comparison . . . . .	21
Initial Climb . . . . .	21
Airspeed control . . . . .	21
Longitudinal stability effects . . . . .	24
Relationship of pitch attitude to airspeed . . . . .	26
Thrust-lever sensitivity . . . . .	28
Lateral-Directional Characteristics . . . . .	29
RESULTS AND DISCUSSION OF CERTIFICATION TASKS . . . . .	30
Three-Engine Takeoffs . . . . .	31
Airplane response to engine failure . . . . .	31
Controlled takeoffs after engine failure . . . . .	32
Engine-out crosswind takeoffs . . . . .	33
Summary of engine-failure studies . . . . .	33
Determination of Minimum Unstick Speed, $V_{MU}$ . . . . .	33
$V_{MU}$ test procedure . . . . .	34
General $V_{MU}$ characteristics . . . . .	34
Effect of speed abuse on low-thrust takeoffs . . . . .	35
Effect of lift loss due to elevator deflection . . . . .	36
Ground Minimum Control Speed . . . . .	38
Simulator results, nose-wheel steering inoperative . . . . .	38
Effect of high T/W on $V_{MCG}$ . . . . .	39
Effect of nose-wheel steering on $V_{MCG}$ . . . . .	39

## TABLE OF CONTENTS - Concluded

	<u>Page</u>
Air Minimum Control Speed . . . . .	40
VMCA test results . . . . .	40
Out-of-Trim Takeoffs . . . . .	41
Takeoff with full nose-down mistrim . . . . .	41
Takeoff with full nose-up mistrim . . . . .	41
PILOT ACCEPTANCE OF THE Y-SHAPED CONTROL WHEEL . . . . .	42
SUMMARY OF RESULTS . . . . .	42
APPENDIX A - LATERAL-DIRECTIONAL DERIVATIVES AS USED IN THE SIMULATOR INVESTIGATION . . . . .	44
REFERENCES . . . . .	45

A PILOTED SIMULATOR STUDY OF TAKEOFF PERFORMANCE  
AND HANDLING QUALITIES OF A DOUBLE-DELTA  
SUPERSONIC TRANSPORT

By C. Thomas Snyder and Charles T. Jackson, Jr.

Ames Research Center

SUMMARY

The takeoff characteristics of a generalized double-delta supersonic transport configuration were investigated in a fixed-cockpit simulator equipped with an external visual display. The objectives were to investigate performance and handling qualities, identify possible problem areas, and assist in the evaluation of certification requirements to be used during the development of the SST.

Comparisons of the takeoff characteristics are drawn between the simulated SST and a reference subsonic jet transport (SJT). The unaugmented SST exhibited: (1) excellent performance during normal takeoffs, (2) a greater probability of nacelle or tail scrapes than the SJT, indicating a need for more time for the rotation maneuver, a longer landing gear on the design tested, or higher lift-off speeds, (3) initial climb characteristics which were acceptable but unpleasant, due to a tendency toward pitch "wandering," aggravated by negative speed-drag stability, (4) good lateral-directional and engine-out characteristics, and (5) a performance sensitivity to lift-off speed abuse during marginal-thrust takeoffs, which indicated the need for review of the present airworthiness criterion regarding one-engine-inoperative first-segment climb.

INTRODUCTION

High-speed flight considerations have resulted in supersonic transport configurations which are radically different from those of the current subsonic jet transports and which will have takeoff and landing characteristics in some ways significantly different from those of the current subsonic jets. Predominant among these differences are:

- (1) Higher gross weights
- (2) Higher thrust-weight ratios
- (3) Low static longitudinal stability
- (4) Long slender fuselages with high pitch and yaw inertias

Additional differences found in the delta-wing configuration include:

- (5) Low roll inertia
- (6) Speed-drag instability during initial climb and landing approach
- (7) Maintenance of usable lift (absence of stall) well beyond conventional stall angles of attack
- (8) High attitude angles during lift-off and the attendant effects upon tail-runway clearance, visibility, and height judgment
- (9) Large ground effects upon aerodynamic lift, drag, and pitching moment.

A program of piloted simulator studies was initiated at the Ames Research Center to investigate the handling qualities, identify possible problem areas, and assist in the evaluation of certification requirements to be used during the development of the SST. As a part of this program, the takeoff characteristics of a fixed-wing, low-aspect-ratio supersonic transport were investigated on a fixed-cockpit simulator and are the subject of the present report. Peculiarities pertaining to the SST takeoff in general were described in references 1 to 3. Of particular concern were the degree of difficulty of controlling speed and flight path during climb immediately after takeoff, the handling qualities and performance following an engine failure, the rotation characteristics, and the effects of longitudinal mistrim. Validation of the simulation for the subject tasks is reported in reference 4, which describes the simulator duplication of the takeoff certification program of a subsonic jet transport.

The findings presented herein should be considered in the light of the trends demonstrated, relative to the subsonic jet, rather than as the evaluation of a particular configuration. The absolute numbers are directly a function of the aerodynamic, geometric, and engine characteristics used in the study, all of which would undergo numerous changes before construction of a prototype; however, the gross trends should remain the same.

Thrust-weight ratios of the subsonic jet transports are continually increasing; thus the performance of the reference subsonic transport in this report does not represent the highest levels found in the commercial fleet today.

The information presented in this report was obtained under conditions related to a certification flight test; it is recognized that airline operational techniques are often quite different. For example, certification considerations influenced the use of rapid rotation rates and a constant-speed initial climb below the minimum-drag speed.

#### NOTATION

AGL	above ground level
ANU,AND	airplane nose up, airplane nose down
$\bar{c}$	wing mean aerodynamic chord, ft

c.g.	center of gravity
$C_D$	drag coefficient, $\frac{\text{drag force}}{qS}$
$C_{L_{\delta_e}}$	$\frac{\partial C_L}{\partial \delta_e}$ , $\text{rad}^{-1}$
$C_m$	pitching-moment coefficient, $\frac{\text{pitching moment}}{qS\bar{c}}$
$C_{1/2}$	cycles to damp to one-half amplitude
D	aerodynamic drag, lb
IFR	instrument flight rules
$I_y$	pitching moment of inertia, slug-ft <sup>2</sup>
L	aerodynamic lift, lb
$L_{\delta_e}$	$\frac{qS}{m} \left( \frac{\partial C_L}{\partial \delta_e} \right)$ , $\frac{\text{ft}}{\text{sec}^2\text{-rad}}$
m	airplane mass
MSL	mean sea level
$M_\alpha$	$\frac{qS\bar{c}}{I_y} \left( \frac{\partial C_m}{\partial \alpha} \right)$ , $\frac{1}{\text{sec}^2}$
$M_{\delta_e}$	$\frac{qS\bar{c}}{I_y} \left( \frac{\partial C_m}{\partial \delta_e} \right)$ , $\frac{1}{\text{sec}^2}$
q	dynamic pressure, $\frac{\rho V^2}{2}$ , lb/ft <sup>2</sup>
RPS	rudder-pedal-actuated nose-wheel steering
S	reference wing area, ft <sup>2</sup>
s.m.	static margin
s <sub>35</sub>	runway distance to clear a 35-foot obstacle
SJT	subsonic jet transport
SST	supersonic transport
T	thrust, lb

$T_{\text{req}}$	thrust required, lb
$V$	equivalent airspeed, ft/sec or knots as noted
VFR	visual flight rules
$V_{\text{LOF}}$	speed at main gear lift-off, knots
$V_{\text{MCA}}$	air minimum control speed, knots
$V_{\text{MCG}}$	ground minimum control speed, knots
$V_{\text{MU}}$	minimum unstick speed, knots
$V_{\text{R}}$	speed at time of rotation control input, knots
$V_1$	takeoff decision speed, knots
$V_2$	takeoff safety speed and three-engine climb speed
$V_{35}$	attained speed at 35-foot wheel height, knots
$W$	gross weight, lb
$\alpha$	angle of attack, radians or degrees as noted
$\beta$	sideslip angle (relative wind from right, positive), deg
$\gamma$	flight-path angle (climb, positive), degrees or gradient in percent as noted
$\Delta$	incremental change
$\delta_a$	average aileron deflection angle (right aileron up, positive), radians or degrees as noted
$\delta_e$	elevator deflection angle (AND, positive), radians or degrees as noted
$\delta_F$	flap deflection angle, deg
$\delta_r$	rudder deflection angle, radians or degrees as noted
$\delta_{\text{ard}}$	roll-damper (aileron) deflection angle, radians or degrees as noted
$\zeta_{\text{sp}}$	longitudinal short-period damping ratio
$\theta$	airplane pitch attitude relative to horizontal (ANU, positive), radians or degrees as noted
$\rho$	air density, slugs/ft <sup>3</sup>
$\phi$	bank angle (right wing down, positive), deg



$\omega_{nsp}$  undamped longitudinal short-period frequency, radians/sec  
( $\cdot$ ) derivative with respect to time,  $\frac{d}{dt}$

### TEST EQUIPMENT

Two general purpose electronic analog computer consoles (providing a total capacity of about 200 operational amplifiers) were programmed to represent the rigid body motion of the airplane in six degrees of freedom. Individual landing gear reactions and the aerodynamic ground plane influence were included in the equations of motion. Limits of the simulation were 0 to 4000 feet altitude (AGL) and 0 to 237 knots equivalent airspeed. In all computations standard sea-level conditions were assumed. The computer program and simulator equipment are described further in reference 4.

The simulator cab consisted of a fixed transport cockpit fitted with a flight test instrument display. Figure 1 shows the instrument display and pilot's view from the cockpit. Basic transport flight instrumentation was augmented by indications of angle of attack, sideslip, sensitive airspeed, normal and longitudinal acceleration, control forces, tail clearance, and lift-off. The five-digit counter mounted above the engine instruments was used for correlating data.



A-32752-5.3

Figure 1.- Instrument display and outside visual scene in takeoff simulator.

The outside-world visual scene was provided by means of a projected closed-circuit television picture (unity magnification) of a model runway. References 4 to 6 further describe the visual presentation and include subjective evaluations.

The pilot's station was equipped with four thrust levers, toe brakes, rudder-pedal nose-wheel steering, a control column shaker (actuated when angle of attack exceeded  $17-1/2^{\circ}$ ) and a pneumatic seat cushion which was pulsed to simulate the passing over the runway divider strips during the takeoff roll and also programmed to provide subtle normal acceleration cues.



A-36158

Figure 2.- Y-shaped control wheel used for delta SST simulator studies.

A Y-shaped control "wheel" (primarily for improved instrument visibility and shown in fig. 2) replaced the conventional transport-type wheel used during the simulation program of the subsonic jet transport. The assumed relationships between control force and displacement (fig. 3) were typical of values being proposed for the SST at the time of the study.

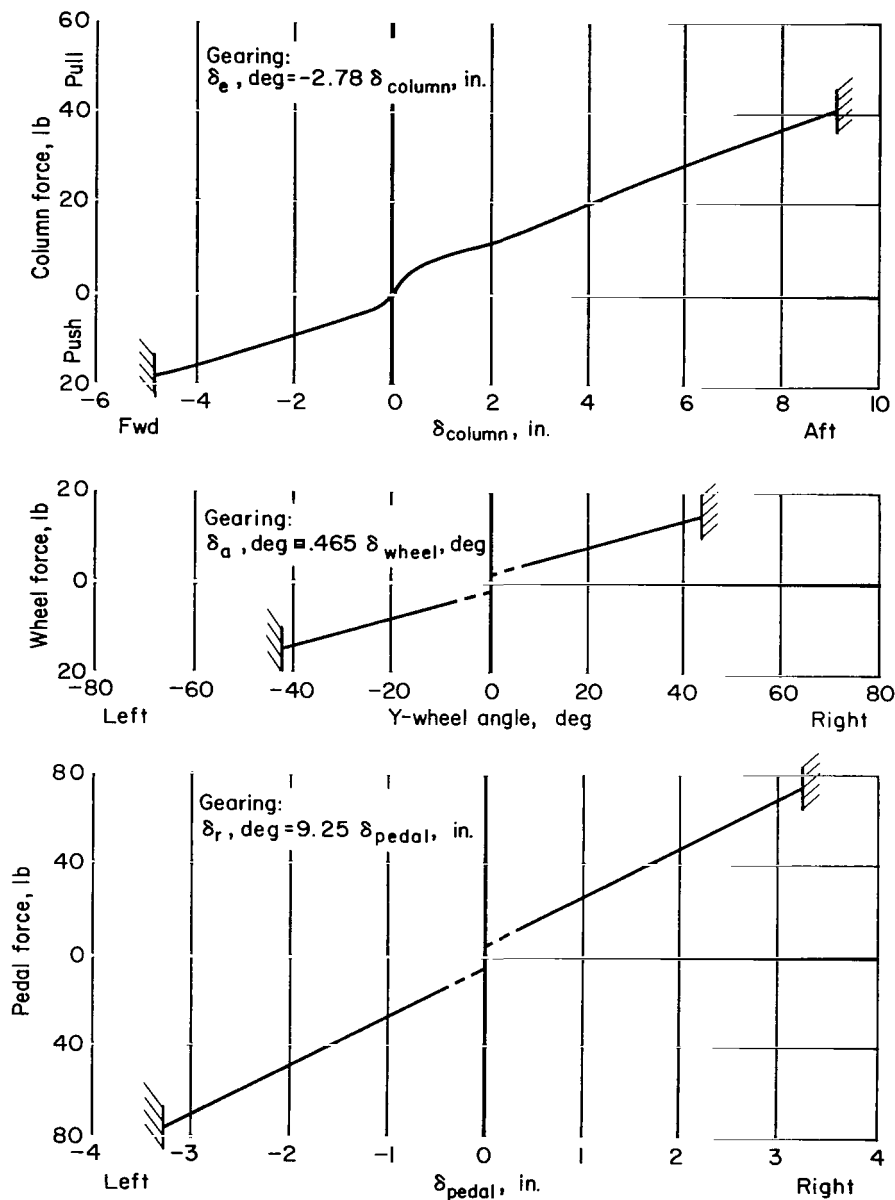


Figure 3.- Control force-displacement characteristics of the simulated SST.

## TEST CONFIGURATION

The supersonic transport studied in this investigation was a generalized low-aspect-ratio double-delta configuration similar to that shown in figure 4. Reference wing area was 7000 square feet, with a mean aerodynamic chord of 74 feet and aspect ratio (of the basic delta) of 1.9. The longitudinal control system employed elevon-type control surfaces. No flaps or other high lift devices were used.

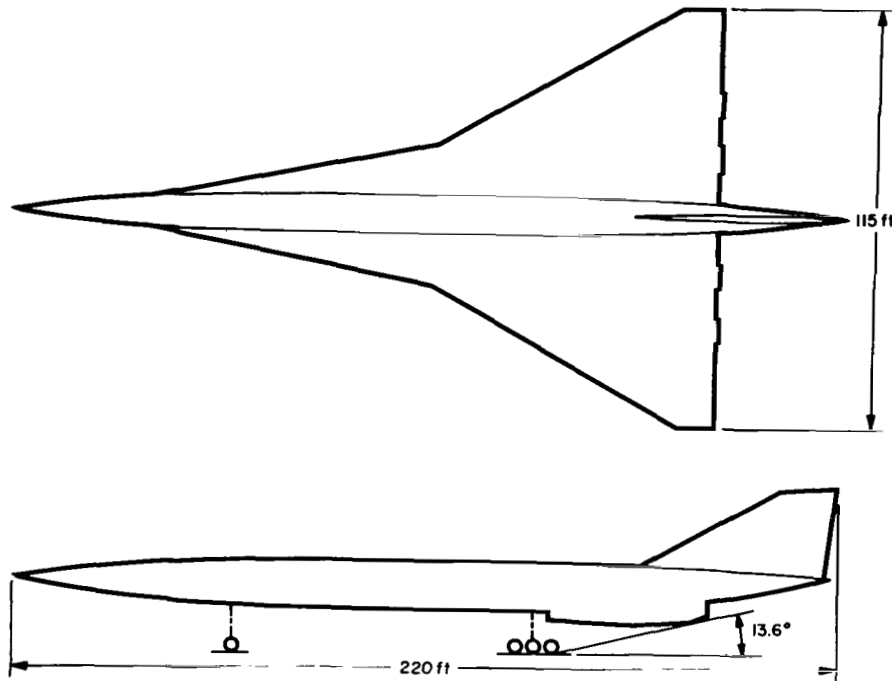


Figure 4.- Two-view sketch of the simulated SST.

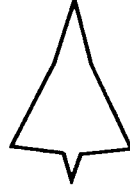
Aerodynamics of the large, tailless delta class of airplane and the corresponding low-speed characteristics are described in references 7 to 9. Table I presents some of the more significant parameters assumed for the study.

Control system characteristics of the simulated SST are described in the discussion of test equipment. All discussion refers to a basic unaugmented airplane except where otherwise stated.

Maximum static thrust of 50,000 pounds per engine was assumed. For any thrust control setting, a thrust lapse with increasing speed (a general characteristic exhibited by turbojet engines in the takeoff speed range) of 15.5 pounds/knot per engine was programmed. For minimum control speed tests, engine dynamic response was represented by a first-order time constant of 2.0 seconds.

TABLE I.- BASIC CHARACTERISTICS OF THE SIMULATED SUPERSONIC  
TRANSPORT COMPARED WITH THOSE OF A SUBSONIC JET TRANSPORT

Double  
delta SST



Subsonic  
jet transport



Gross weight, lb	450,000		300,000
Maximum T/W	0.44		0.21
Wing loading, W/S, lb/ft <sup>2</sup>	64		107
Roll inertia, slug-ft <sup>2</sup>	$2.5 \times 10^6$		$5.7 \times 10^6$
Pitch inertia, slug-ft <sup>2</sup>	$21 \times 10^6$		$4.0 \times 10^6$
Yaw inertia, slug-ft <sup>2</sup>	$24 \times 10^6$		$9.5 \times 10^6$
Static margin, $-dC_m/dC_L$	0.02	0.04	0.21
$M_\alpha$ at $V_{LOF}$ , 1/sec <sup>2</sup>	-0.156	-0.312	-1.375
$\omega_{n_{sp}}$ at $V_{LOF}$ , rad/sec	0.68	0.78	1.30
$\zeta_{sp}$ at $V_{LOF}$ , 1/sec	0.94	0.81	0.52
$M_{\delta_e}$ at $V_{LOF}$ , 1/sec <sup>2</sup>	-0.75	-0.75	-1.26
$L_{\delta_e}$ at $V_{LOF}$ , ft/sec <sup>2</sup> -rad	37.8	37.8	7.6

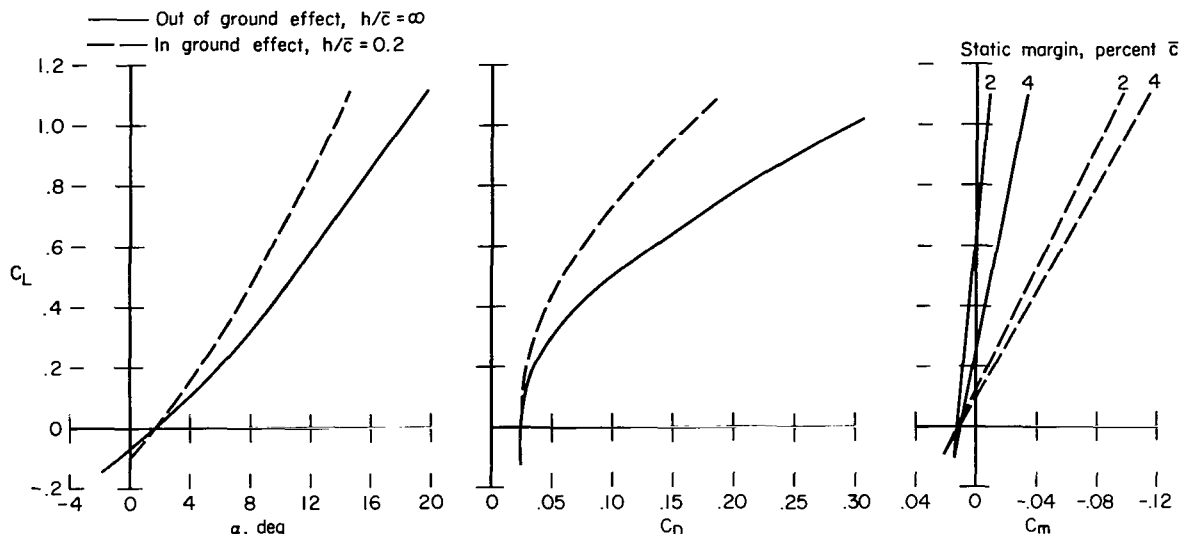


Figure 5.- Lift, drag, and pitching-moment characteristics assumed for the simulated SST; landing gear extended.

Lift, drag, and pitching-moment characteristics used are presented in figure 5 - with the influence of ground proximity indicated. Ground effect has a greater influence on the characteristics of the low-aspect-ratio wing (refs. 7-11) than on the moderate aspect ratios representative of the subsonic jets. The height factor used for transition from the "on-ground" to "out-of-ground effect" values is shown in figure 6. Constant values of  $C_{m\delta_e}$  and

$$(\Delta C_i)_{GE} = H.F. \times [(C_i)_{h/c=0.2} - (C_i)_{h/c=\infty}] ; i = L, D, m$$

$C_{L\delta_e}$ , corresponding to "on-ground" estimates, were used during the majority of the simulator runs. In a number of takeoffs near the conclusion of the test series, these values were decreased to 76 percent of their "on-ground" values as the airplane climbed out of ground effect, with no significant differences noted in flying characteristics.

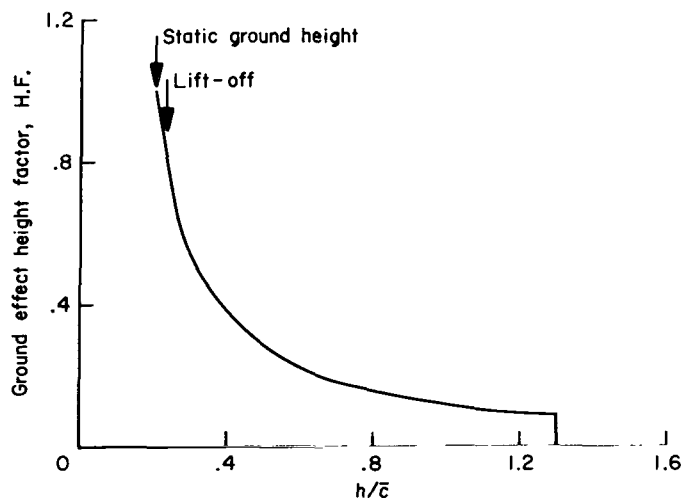


Figure 6.- Height factor used for transition from "on-ground" to "out-of-ground" effect ( $h$  = quarter-chord height here).

## TEST PROCEDURE

The simulator tests were conducted in much the same manner as an actual flight test certification program. Flight cards describing the task and calling out areas of interest were provided the pilot during a briefing session before he entered the cockpit. Pilots were allowed a number of familiarization runs each time they entered the simulator.

Five test pilots participated in the study, representing NASA (2), FAA (1), and an airframe manufacturer (2). Two of the pilots had participated in the flight test certification program of a subsonic jet transport and four of the pilots had taken part in the trial certification program for validating the simulator (ref. 4). All pilots had experience in high-performance aircraft.

Takeoffs were made at two basic thrust settings; one provided maximum available thrust (assumed 50,000 lb static thrust per engine) and one provided less than maximum thrust (assumed 39,550 lb static thrust per engine) as might be required in order to minimize airport and community noise. During the noise-abatement takeoffs, thrust was reduced to the minimum duct burning level (assumed 28,200 lb at 180 knots) at 850 feet above ground. Aspects of the airport noise problem are discussed in references 12 and 13.

Elevator trim for takeoff was set to produce zero force at the four-engine climb speed. Landing gear retraction was initiated approximately 4 seconds after lift-off. Table II contains the takeoff reference speeds assumed for the investigation. These values were based on a manufacturer's estimates for a similar configuration.

TABLE II.- TAKEOFF REFERENCE SPEEDS

$V_1$ . . . . .	$V_R$	
		<div style="display: flex; align-items: center;"> <div style="font-size: 3em; margin-right: 10px;">{</div> <div> <div>152 knots    Used for takeoff profiles and initial runs</div> <div>141 knots    Used for takeoffs during latter part of program, especially at maximum T/W. See discussion of rotation speed selection.</div> </div> </div>
$V_{LOF}$ , target . . . . .	169 knots	
$V_2$ , $V_{climb}$ (3 engine). . . . .	176 knots	
$V_{climb}$ (4 engine). . . . .	180 knots	

## RESULTS AND DISCUSSION OF BASIC TAKEOFF CHARACTERISTICS

Various characteristics of the airplane during takeoff are presented in detail, with consideration given to the effects of variations in technique that are representative of those observed in service operation. The successive segments of the takeoff - ground roll, rotation, transition, and initial climb - are treated separately.

### Ground Roll

Although not surprising, one of the most striking features of the SST takeoff is the high acceleration during the ground roll, which is simply a result of the high thrust-weight ratio ( $T/W$ ) required for supersonic flight. Besides reducing takeoff distances, this high acceleration allowed the pilot much less time for takeoff monitoring and decision making. (At maximum gross weight and maximum thrust, time from brake release to  $V_R$  was approximately 19 seconds, compared to 50 seconds for the subsonic jet transport.) Pilot comments reflected no concern with the shorter times; however, it is not known to what extent operational factors that were missing and motion cues would affect their response. Many high-performance aircraft now in operation have comparable takeoff acceleration.

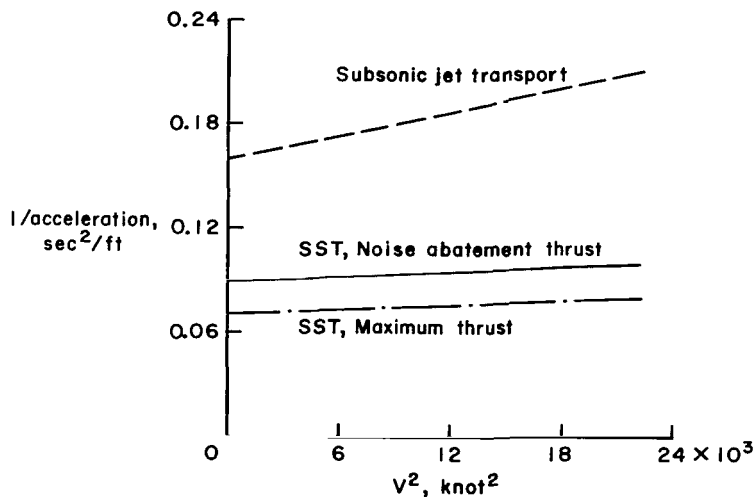
In figure 7 the longitudinal acceleration of the SST is compared to that of the subsonic jet transport. In the taxi attitude, the SST has approximately twice the acceleration of the SJT (fig. 7(a)). The degradation in acceleration with increasing speed is less pronounced in the SST because of the lower drag-weight ratio in the taxi attitude.

### Rotation

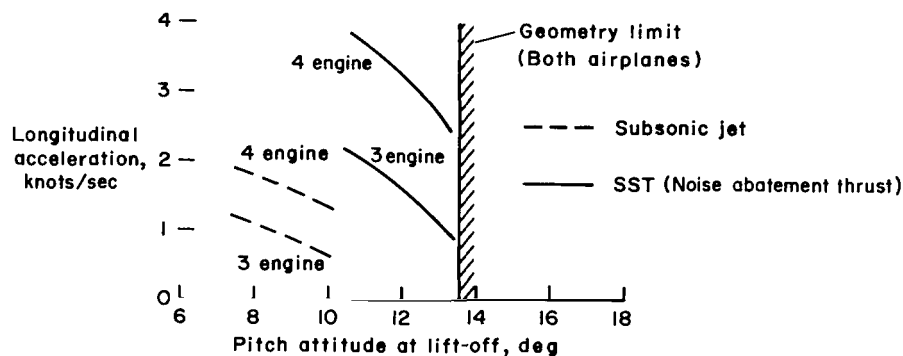
A number of factors associated with the rotation appeared significantly different between the simulated SST and the subsonic jet transport. Among these were the effects of high pitch attitudes at lift-off, the effect of high longitudinal acceleration on selection of rotation speed  $V_R$  and the resulting lift-off speed, the effects of attitude limitations due to geometry, and the effects of variations in pitch attitude and rotation speed on takeoff distance.

Effect of high pitch attitude on longitudinal acceleration. - Concern over high pitch attitudes at lift-off stemmed from early experience with subsonic jet transports when it was found that a significant increase in takeoff distance resulted from overrotation and the attendant high drag at large angles of attack (ref. 14). In figure 7(b) the acceleration of the SST in the rotated attitude at noise abatement thrust is compared with that of the reference SJT. With three engines operating at the noise-abatement level and the airplane at normal lift-off attitude ( $11^\circ$ - $12^\circ$ ), the SST demonstrated approximately the same acceleration as the SJT during normal lift-off with four engines operating at full thrust. Because of the induced drag effects, SST acceleration was more sensitive to variations in lift-off angle of attack,





(a) Four-engine acceleration, taxi attitude



(b) Acceleration remaining after takeoff rotation

Figure 7.- Comparison of the longitudinal acceleration of the simulated supersonic transport with that of a subsonic jet transport. Gross weights: SST 450,000 lb; SJT 300,000 lb.

as indicated by the steeper slopes. However, even when rotated to the geometric limit, SST acceleration did not fall below the minimum levels of the SJT. The general indications of the tests were that, with the generous thrust margin available and the greater angle-of-attack margin from a severe drag rise, the high pitch attitudes required in takeoff presented no acceleration problems for the SST.

Effect of high acceleration on  $V_R$  and  $V_{LOF}$ . - Before the simulator results are examined, it seems appropriate to consider the effects of the high T/W on the selection of rotation speed,  $V_R$ , and on lift-off speed,  $V_{LOF}$ . The selection of rotation speed depends directly upon rotation time and longitudinal acceleration. The predicted speed increase during the rotation maneuver (based on the T/W and an assumed rotation time) is subtracted from the desired lift-off speed (target  $V_{LOF}$ ) in order to determine  $V_R$ . This speed margin between  $V_R$  and  $V_{LOF}$  is based on three-engine acceleration

(ref. 15), primarily to avoid lift-off below the target value in the event of an engine failure. Consequently, four-engine lift-off speeds are somewhat higher than the target value.

The higher  $T/W$  of the SST causes:

1) A larger speed margin between  $V_R$  and  $V_{LOF}$  (14-19 knots for the SST as compared to 6-7 knots for the SJT, based upon three-engine acceleration and a 4-second rotation time),

2) Greater lift-off speed dispersion (lift-off speeds ranged from 163-179 knots during the simulator four-engine noise-abatement takeoffs),

3) Higher four-engine lift-off speeds (SST four-engine lift-off speeds are 6-7 knots above three-engine lift-off speeds, as compared to 2-3 knots for the SJT. If a cautious 6-second rotation were performed in the SST at maximum thrust, the four-engine lift-off speed could be as high as 190 knots, 21 knots above the target  $V_{LOF}$ ).

Because of the increase in  $L/D$  with increasing speed, the aerodynamic effects of the higher lift-off speed are favorable. However, unfavorable operational considerations may exist (e.g., tire limit speeds, etc.), which are beyond the scope of this report.

Rotation characteristics; ground clearance before lift-off.- In the simulator, a combination of items contributed to the requirement that the margin between  $V_R$  and  $V_{LOF}$  be considerably larger for the SST than for the SJT. These were (1) high longitudinal acceleration, (2) unfavorable unaugmented-airplane pitch dynamic characteristics, (3) high lift-off pitch attitudes, and (4) low margin of ground clearance.

During initial familiarization flights in the SST simulator, pilots tended to use rapid rotation rates. These rapid rotations combined with the low pitch attitude margin ( $1^\circ$  to  $3^\circ$  between normal lift-off and nacelle-strike attitudes, considerably less than the  $4^\circ$  to  $7^\circ$  margin of the subsonic jet transport) caused frequent nacelle strikes. High pitch inertia and difficulty in reading precise angles from the pitch attitude indicator aggravated this tendency. The sluggish pitch response caused difficulty in establishing a desired pitch attitude; consequently, numerous overshoots occurred.

In the simulator, pilots obviously had little reason to fear the nacelle or fuselage contacting the ground. In addition, one pilot commented that the absence of cockpit motion cues made judging the maneuver more difficult. It seems likely that the feedback provided by motion cues would slow the rotation rates and cause more conservative takeoffs. While validating the simulator (ref. 4), the pilots tended to fly the simulator less conservatively than they would an actual flight vehicle.

In an attempt to assess the effect of the missing motion cues and the artificial environment, rotation times and lift-off attitudes from the simulator are compared to those from preliminary XB-70 flight test results (which

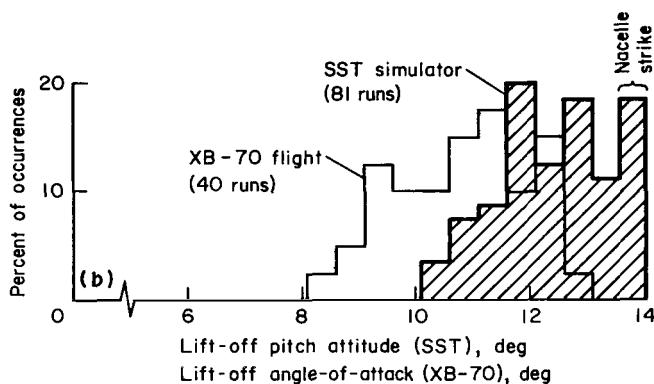
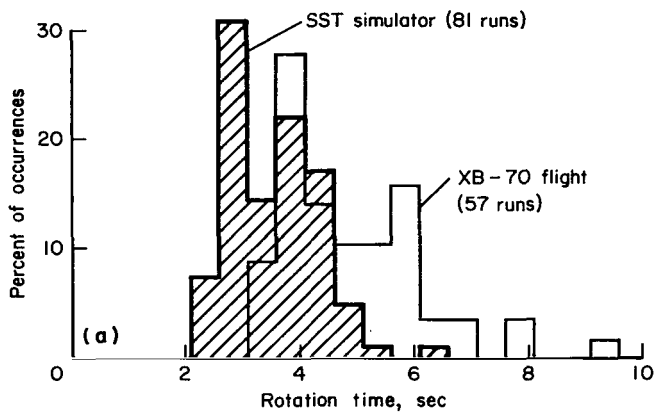


Figure 8.- Comparison of simulated SST takeoff characteristics with preliminary XB-70 flight test values.

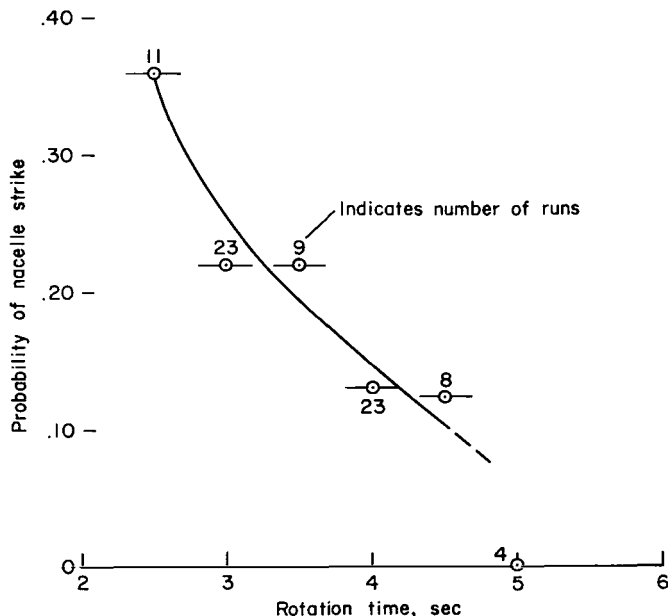


Figure 9.- Probability of nacelle strike versus rotation time for the simulated delta SST;  $0.34 \leq T/W \leq 0.44$ .

are not completely representative of certification maneuvers). The histograms in figure 8(a) show similar profiles, with XB-70 rotation times approximately 1 to 1.5 seconds longer than SST times. The XB-70 rotation times have tended to increase as experience with the airplane increases, a characteristic observed in the SST simulator. In general these observations suggest that realistic rotation times for the delta SST may be on the order of 4 to 6 seconds. (Average certification-flight-test rotation time for the reference SST was approximately 3.5 sec and operational values are nearer to 5 sec.)

Comparative histograms for lift-off attitude are shown in figure 8(b). Again, the distribution and overall band widths are similar. Note that the XB-70 data were obtained from the angle-of-attack sensor; conversion to pitch attitude would likely shift these data  $0^\circ$  to  $0.6^\circ$  to the right. In addition, operational lift-off  $C_L$  for the XB-70 was lower than the SST value (XB-70 takeoff speeds were considerably higher), thereby contributing to the lower takeoff attitudes shown for this vehicle.

Probability of nacelle strike has been plotted against rotation time in figure 9, based upon the fixed-cockpit simulator results. Although 78 runs represent a small quantity for statistical purposes, they show a definite trend of decreasing probability with increasing rotation time. With a 4-second rotation time, the likelihood of a nacelle strike was about

15 percent for the SST design tested. Extrapolation indicates that rotation times on the order of 5.5 seconds would reduce the probability to near-zero.

In addition to the requirement for longer rotation times, two recommendations are apparent. First, protection should be designed into the aircraft against structural damage resulting from a nacelle or tail strike. Secondly, pilots assigned to fly the SST should become familiar with the rotation characteristics in a simulator (with motion, if possible) prior to encountering them in the actual flight situation.

Probability of nacelle strike could also be reduced by lengthening the landing gear or by use of lower normal lift-off attitudes. Either technique requires consideration of additional factors (weight, drag, ground effect, high lift-off speeds, etc.), trade-offs of which prevent simple conclusions.

There was no tendency for the nacelles to strike the ground after the main gear left the ground. For additional discussion, see section entitled Transition.

Incompatibility with present airworthiness criteria.- During the early simulator testing including the noise-abatement series, the primary  $V_R$  speed for the takeoffs was 152 knots. Later, for maximum-thrust takeoffs,  $V_R$  was reduced to 141 knots to allow more time for the rotation. This speed appeared to provide a good spread between  $V_R$  and  $V_{LOF}$ , allowing smooth rotations with lift-offs near 169 knots.

In retrospect, however, the reduced  $V_R$  (141 knots) did not satisfy the present airworthiness criteria which requires that the  $V_R$  speed be not less than a speed which, if the airplane is rotated at its maximum practicable rate, will result in a lift-off speed  $V_{LOF}$  not less than 110 percent of  $V_{MU}$  in the all-engines-operating condition nor less than 105 percent of  $V_{MU}$  in the one-engine-inoperative condition (ref. 16, par. 25.107(e)).

Thus, review of the preceding sections reveals the following dilemma, if high lift-off speeds are to be avoided. SST pitch dynamics and ground clearance considerations encourage slow rotations. These slow rotations combined with high  $T/W$  (high acceleration) result in a large speed difference between  $V_R$  and  $V_{LOF}$ . To satisfy the airworthiness criterion mentioned above, which safeguards against lift-off too near  $V_{MU}$  if the airplane is rotated abruptly,  $V_R$  must be near or greater than  $V_{MU}$ . This, then, results in high lift-off speeds (considerably above those for the SJT) in the case of slow conservative rotations which are likely to be typical of airline operational procedure.

Perhaps some relaxation of this criterion would be possible, allowing use of lower  $V_R$ , if assurance could be provided against the occurrence of an abrupt rotation, or if the consequences of lift-off near  $V_{MU}$  were acceptable. Note that this dilemma arises primarily when acceleration levels are high; thus lift-off near  $V_{MU}$  does not appear as critical as with the SJT. Use of a takeoff director might aid in providing more consistent rotations, and be a step in the direction away from the abrupt rotation. Additional study of this topic is needed.

Effects of abnormal rotations.- In operation, rotation speed and lift-off attitude may vary considerably. Figure 10 (from ref. 17), derived from flight records of a subsonic jet transport in normal scheduled service, indicates the range of variations actually experienced. Rotation speeds vary 10 to 15 knots from the target value and attitudes cover a range from  $3\frac{1}{2}^\circ$  below to  $2^\circ$  above the target unstick attitude. Variability in the achieved rotation speed for the noise-abatement-takeoff simulator runs is shown in figure 11, indicating rotations falling generally from 6 knots below to 3 knots above the target speed. Rotation was initiated 10 knots below  $V_R$  during one run.

(Observed in normal scheduled service)

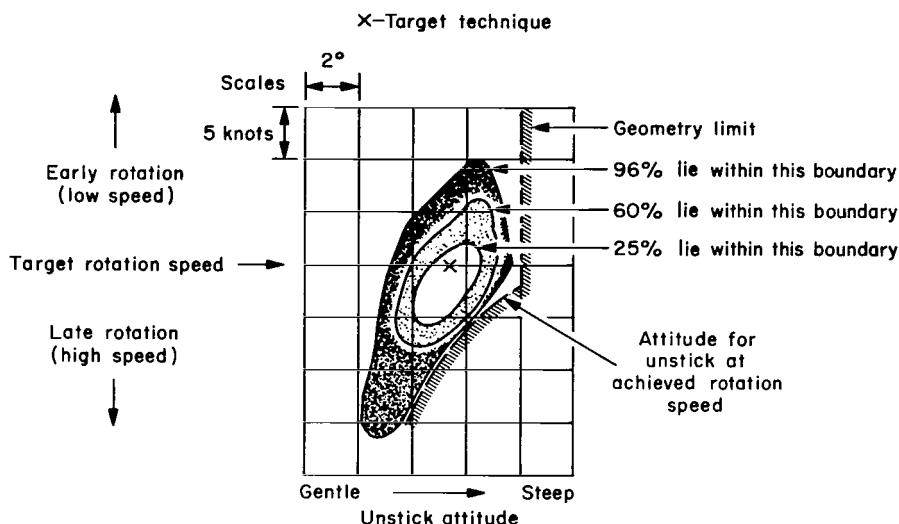


Figure 10.- Relation between achieved rotation speed and unstick attitude for a subsonic jet transport as observed in normal scheduled service (ref. 17).

- 30 - Notes: 1. Sensitive airspeed indicator used.  
Scale 100 knots/revolution  
2. Sample size - 55 runs

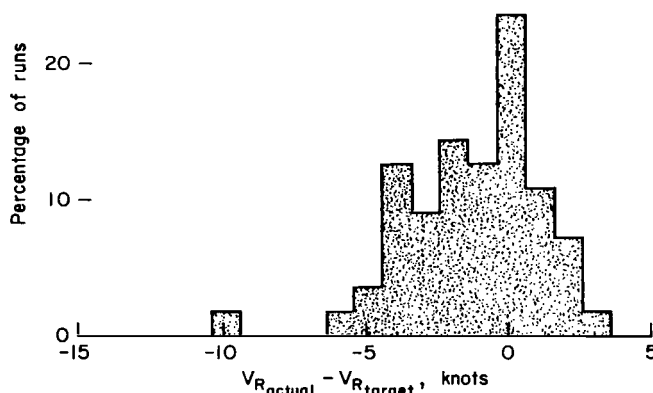


Figure 11.- Histogram of achieved rotation speed from the noise-abatement takeoffs performed with the delta SST simulation; static  $T/W = 0.34$ .

Accordingly, the effects of overrotation, underrotation, and early and late rotation on takeoff distance were investigated on the analog computer (nonpiloted) and the results are shown in figure 12. Overrotation in this sense refers to rotation to angles of attack beyond those normally used for

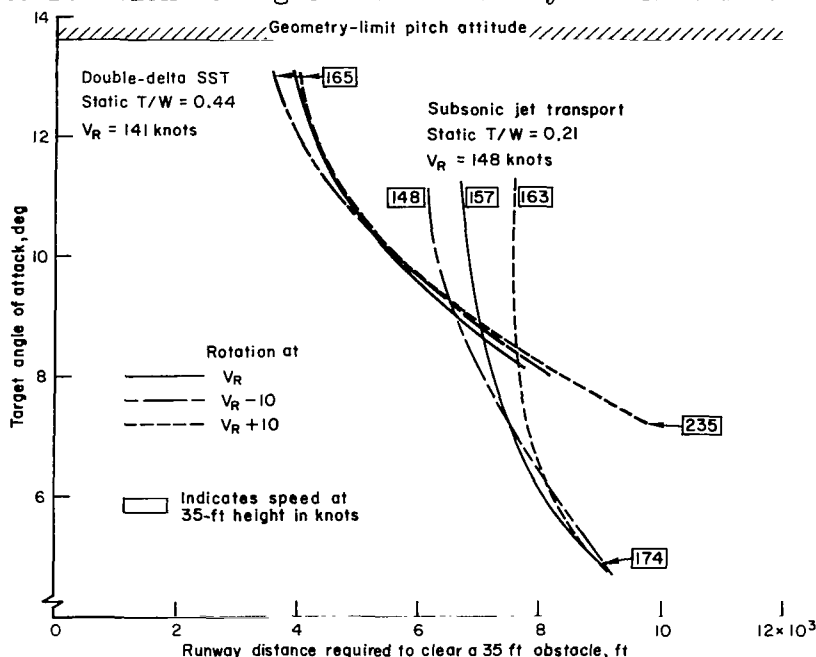


Figure 12.- Effect of overrotation, underrotation, and early and late rotation on takeoff distance. Maximum thrust takeoffs, sea-level standard conditions. Analog computer runs, procedure: rotate at the indicated speed to target  $\alpha$  with normal rotation rate ( $\approx 2.5^\circ$  to  $3^\circ/\text{sec}$ ) and maintain this  $\alpha$  until 35-foot height reached.

lift-off. The heavy family of curves represents SST takeoffs at maximum thrust. Shown for comparative purposes are the results of a similar set of computer runs conducted with the subsonic jet transport simulation. At the higher angles of attack where the curves diverge, lift-off occurred prior to or immediately as the target  $\alpha$  was reached. Where the curves group close together, airspeed was not high enough for lift-off when the target  $\alpha$  was reached so the ground run continued in the rotated attitude until airspeed had increased sufficiently for lift-off. Because of the test technique of maintaining constant angle of attack through the 35-foot altitude, airspeed varied considerably at the 35-foot point. The extreme values are shown in the boxes of figure 12.

Two differences between SST and SJT results are immediately apparent; SST takeoff distance is more sensitive to variations in target angle of attack and is less sensitive to variations in the speed at which rotation is initiated. Increased rotation angles and overrotation of the SST resulted in shorter takeoff distances while underrotation significantly extended the ground run; underrotation of  $3^\circ$  extended takeoff distance by 2800 feet for the SST and 1100 feet for the SJT. Rotation of the subsonic jet beyond  $9^\circ$  to  $10^\circ$  does not provide much of a reduction in takeoff distances (and although not shown by the figure, if  $C_{L_{\max}}$  were exceeded, takeoff distance would be significantly increased); whereas with the SST, significant reductions are possible up to

near the geometry limit. This indicates that delta SST aircraft may be operated as near as practical to the geometry limit when field length is marginal.

### Transition

Ground clearance after lift-off.- Reference 18 points out the possibility that, for large slender aircraft, the tail may strike the ground well after the instant the main wheels leave the ground, the lowest tail clearance occurring between 1 and 2 seconds after lift-off. This conclusion was based on an analysis in which vertical velocity of the c.g. was assumed to be zero at the instant of lift-off.

Actually,  $\dot{h}$  at lift-off is not zero because the landing gear extends 1-1/2 to 2 feet as it unloads before lift-off occurs. The simulated SST, with its low wing loading and short tail (nacelle) arm, did not tend to strike the nacelles on the ground following lift-off. Departure from the ground was brisk as shown in figure 13 where climb rate is plotted versus time from lift-off. Notice that, at the instant of lift-off, climb rate was 2 to 3.5 ft/sec and increased sharply to over 10 ft/sec within the first second. The brisk rate of departure from the ground was attributed to the high T/W and to the elevator lift regained as the controls were returned toward the trim position.

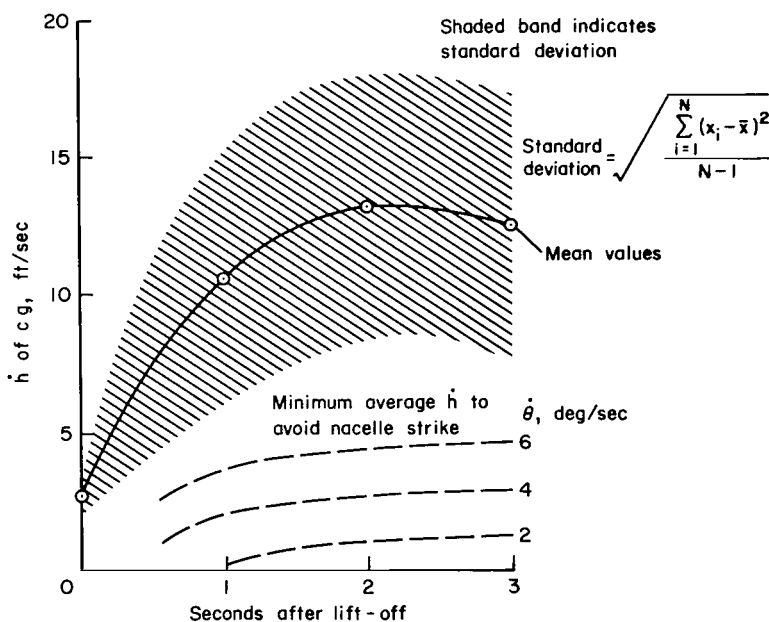


Figure 13.- Takeoff transition; climb rate versus time from lift-off. Noise-abatement takeoffs of simulated SST.

Also shown in the figure are the results of hand calculations to determine the minimum average  $\dot{h}$  necessary to avoid nacelle strike, based upon an assumed constant rotation rate and geometry of the simulated SST. For example, with a  $6^\circ/\text{sec}$  constant rotation rate (this represents rapid rotation), an average  $\dot{h}$  of 3.7 ft/sec would cause the nacelles to strike 1 second after lift-off.

Comparison of the performance of the simulated SST (shaded region) with the hand-calculated minimum values (loci of which are represented by the broken lines) shows that nacelle strike after lift-off is unlikely.

Transient characteristics leaving ground effect.- During normal takeoffs (at maximum or noise-abatement thrust), the aerodynamic transients introduced by leaving ground effect created no problems. It was anticipated that the decrease in static stability that occurs as the airplane leaves ground effect (fig. 5) could cause an objectionable nose-up pitching moment. The various time histories presented later in the report show, however, that this moment performs a subtle, but useful function. With the high  $T/W$  of the SST, the pilot desires to continue to pitch up  $8^\circ$  to  $14^\circ$  past the lift-off attitude during the transition. In this regard the ground effect moment actually assists the pilot.

The loss of ground-effect lift, approximately one-third total lift at lift-off, was not noticed during takeoffs at normal lift-off speeds, with thrust settings providing second segment  $(T - D)/W$  values ranging from 0.26 to 0.07. However, during takeoffs near minimum unstick speed at low thrust settings, it was necessary to accelerate before climbing out of ground effect. This is discussed in greater detail in the section on  $V_{MU}$  determination.

Effect of thrust setting on takeoff distance.- As indicated previously, the SST may use reduced thrust levels during takeoff for noise abatement purposes. Figure 14 presents takeoff distance versus thrust-weight ratio for the 450,000-pound SST, showing that SST takeoff performance exceeds that for the reference SJT even at the reduced thrust levels. At maximum thrust (static  $T/W = 0.44$ ) and sea-level standard conditions, the SST required 4,200 feet to clear a 35-foot obstacle, less than one-half the distance required by the

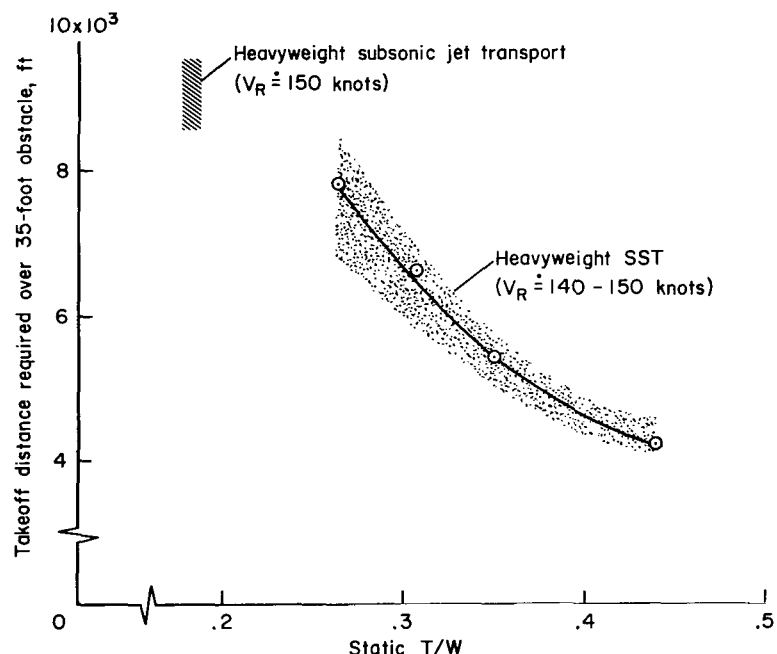


Figure 14.- Effect of thrust setting on four-engine takeoff performance of the simulated supersonic transport. Gross weight: 450,000 lb; standard day.



reference SJT at maximum thrust and gross weight. At the noise-abatement thrust level assumed for the simulator tests (static  $T/W = 0.35$ ), average takeoff distance was 5,400 feet.

Takeoff time history comparison.- Comparable simulator time histories of SST and SJT takeoffs are shown in figure 15, demonstrating, among other things, the influence of the SST's high thrust-weight ratio. Note the higher acceleration, higher pitch attitude after lift-off, and shorter distance and time to a 35-foot altitude for the SST. Lift-off occurred 24 knots after rotation was started, and provided a nacelle clearance of about 1.6 feet.

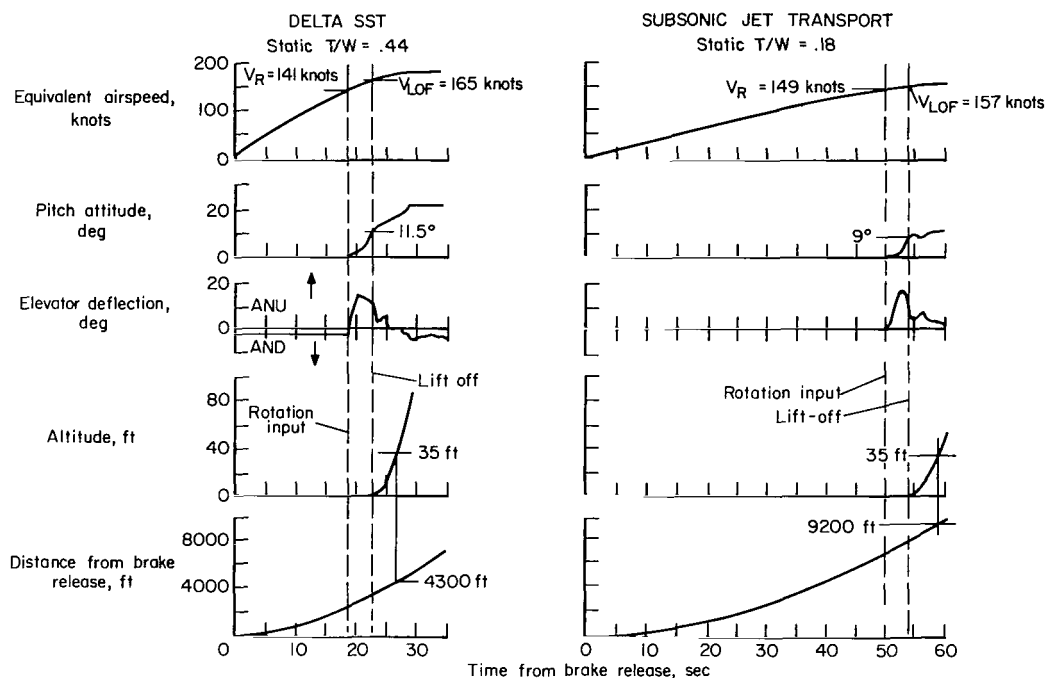


Figure 15.- Comparison of representative takeoff time histories.

### Initial Climb

Airspeed control.- Because of field length and obstacle clearance considerations, initial climbout speeds for the simulated SST were below the minimum drag speed. Hence, special attention was focused on airspeed control during climb on the back of the thrust-required curve; the slope  $(d/dV)(T_{req}/W)$  was -0.0018 per knot at the four-engine climb speed of 180 knots. (During operational takeoffs when field length, obstacle clearance, and noise are not critical, it is likely that some of the initial climb capability will be used for accelerating to speeds that will yield more efficient lift-drag ratios. For example, see the increase in flight-path angle with increasing speed in fig. 19). This negative slope of the thrust-required curve has a different effect on climbout than on landing approach because of the different techniques employed. During an approach, pitch attitude and thrust are adjusted

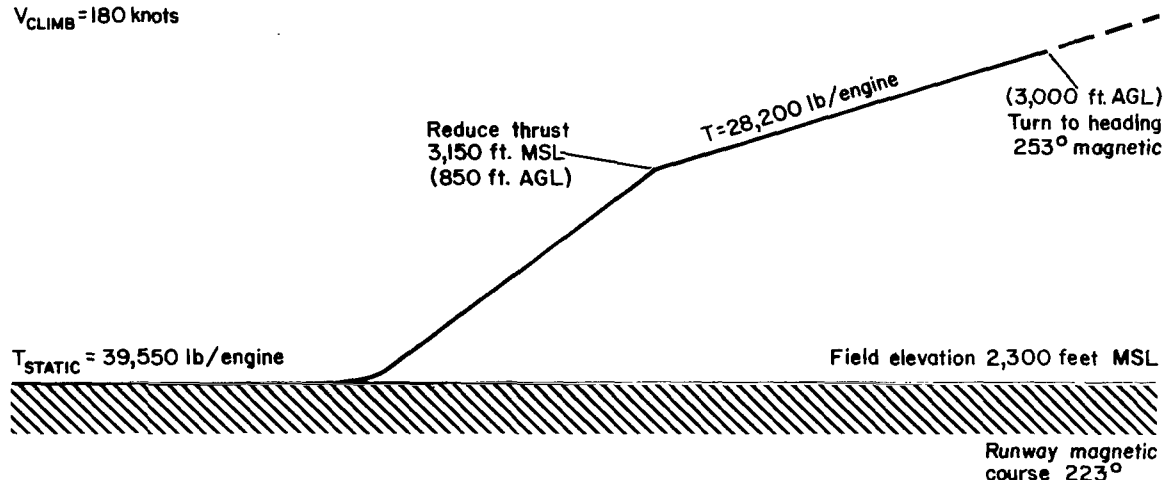
to maintain the desired flight path and target speed. For the climb the thrust setting is fixed, leaving only the pitch control for maintaining airspeed and flight path. Any deviation from the target climb speed is accompanied by a deviation in flight path, resulting in a decrease in the steady-state climb gradient as airspeed becomes low.

Fifty-four noise-abatement takeoff profile runs (see sketch below) were completed in order to evaluate the initial climb characteristics. The simulator task required that the pilot accurately control speed, reduce power at 850 feet above ground level for noise abatement, and maintain alignment with the localizer backcourse; no additional communication or navigation tasks were included.

$V_I = V_R = 152$  knots

$V_{LOF} = 169$  knots

$V_{CLIMB} = 180$  knots



Runs were made under both IFR and VFR conditions in smooth air. To provide some disturbances, rough air in the form of relatively long-term vertical drafts with peak amplitudes of about 30 ft/sec were introduced into the longitudinal mode for some of the takeoffs. Effects of these vertical drafts tended to be masked by the limitations of the fixed-cockpit simulation; that is, the pilots' control inputs were not modified by physical disturbances associated with the turbulence.

Time histories for two representative runs (VFR) are shown in figure 16, which includes the vertical draft profile. The flight path and airspeed were generally controlled in a satisfactory manner. Some pilots reported increased difficulty in maintaining the desired airspeed in comparison with the SJT, while others reported no difficulty but observed that increased attention was devoted to airspeed control. (Much of the difficulty experienced was attributed to the pitch attitude control problems discussed in the following section.) No significant additional difficulty in controlling airspeed was reported due to the rough air environment or with zero static margin.

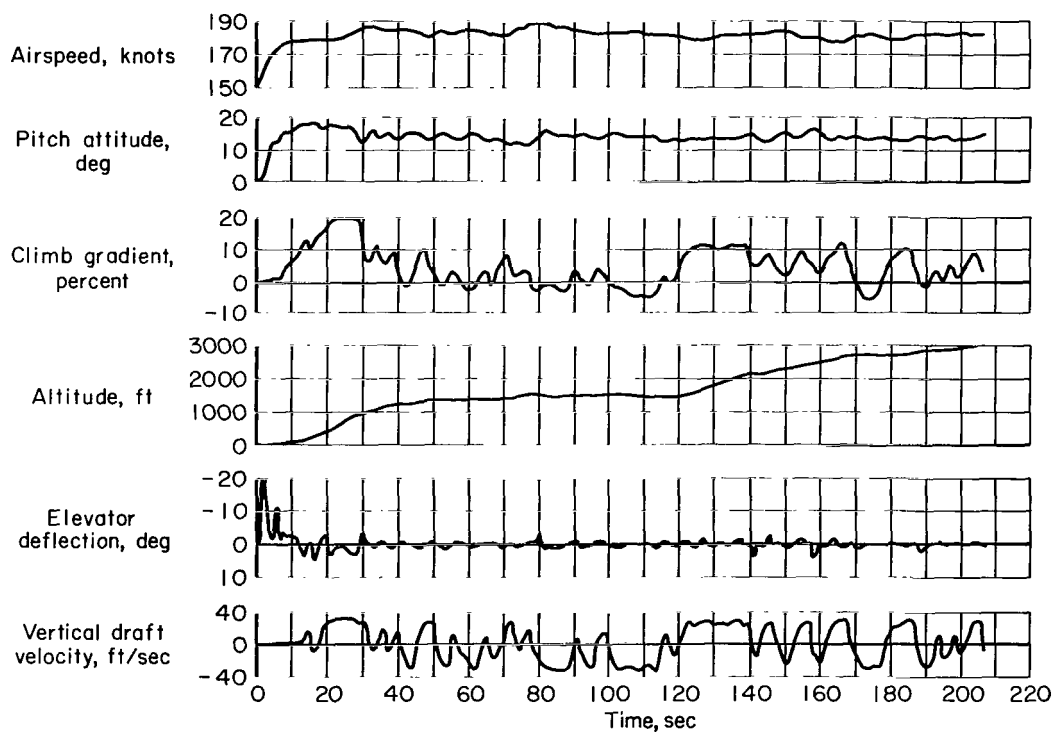
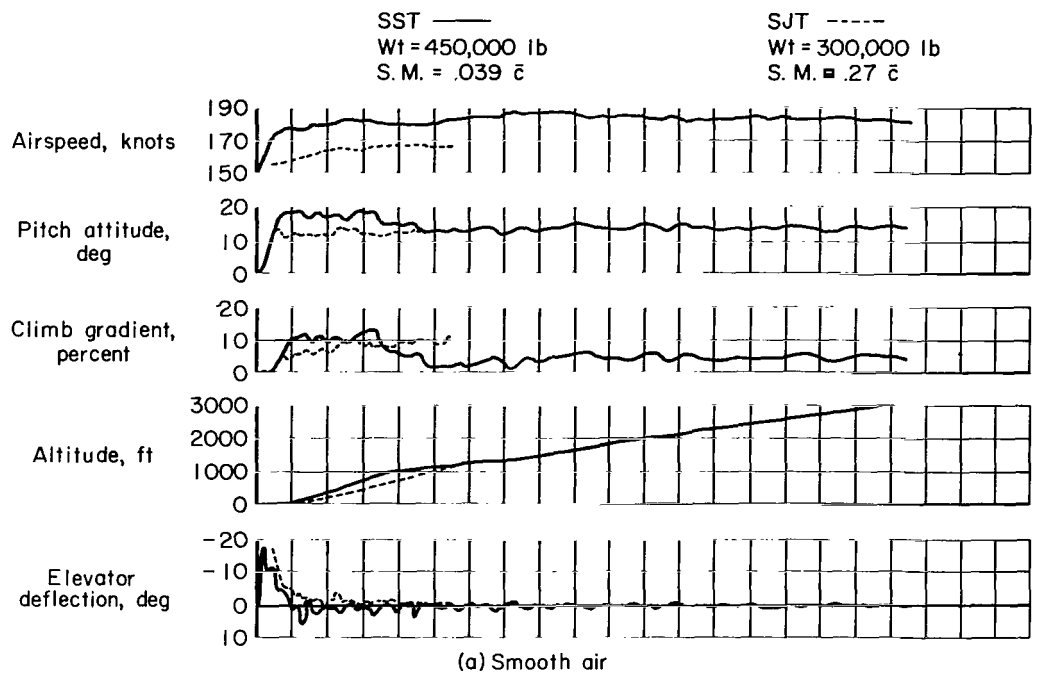


Figure 16.- Time histories of delta-SST noise-abatement takeoff climb profiles performed in the fixed-cockpit simulator.

Table III summarizes the general range of maximum airspeed deviations from the target value during the initial-climb tests.

TABLE III.- MAXIMUM AIRSPEED DEVIATIONS DURING INITIAL CLIMB

Condition	Pilot	Number of runs	General range of maximum values, knots	Extremes reached, knots
Smooth air, VFR	A	8	+5 to -4	+6, -5
	B	3	+10 to -5	+12, -10
Smooth air, IFR	A	14	+6 to -5	+9, -15
	D	15	+7 to -11	+20, -20
	C	4	+10 to -5	+20, -10
Vertical drafts, VFR	A	7	+9 to -9	+15, -10
	B	3	+4 to -8	+4, -11

Longitudinal stability effects.- Pitch attitude control was considered marginally satisfactory. Pilots reported that pitch attitude and rate of climb tended to "wander"; small pitch attitude corrections resulted in overshoots and a continual "hunting" for the desired attitude. This characteristic has been predicted for aircraft having a low short-period natural frequency and high damping and is discussed at length in references 19 and 20 ( $\omega_{nsp}$  and  $\zeta_{sp}$  were 0.7 to 0.8 rad/sec and 0.8 to 0.9, respectively, for the simulated unaugmented SST). In the studies described in reference 19 pilots complained of sluggishness or slow response. They reported that the response kept building after they had expected it to stop, leading them to overcorrect, and consequently produce a pilot-induced oscillation. This oscillatory tendency is evident in the pitch attitude and climb gradient traces of figure 16. A time history, taken from the simulator records of a subsonic jet transport climbout, is shown for comparison. The increased difficulty in controlling SST pitch attitude is indicated by comparing the pitch attitude and elevator traces for the two airplanes. Reference 20 concluded that when the short-period frequency is less than about 1.6 rad/sec, the airplane does not readily maintain angle of attack or attitude by itself; the pilot must constantly provide stabilization and, moreover, he must overdrive the airplane to obtain satisfactory attitude response. In addition, it was concluded that short-period dynamic characteristics which reduce the precision of pitch attitude control will consequently degrade the precision of flight-path and airspeed control. Results of the present tests corroborate these trends.

In the present study, one pilot commented that it was difficult to "lock on" the target speed, but that it was easy to hold airspeed once it was stabilized. With full attention the pilot could maintain airspeed within  $\pm 3$  to 4 knots. However, with distractions, such as the power reduction at 850 feet AGL, airspeed deviations could be surprisingly rapid. There was very little noticeable trim change due to thrust and little apparent change in stick force

to warn the pilot of an off-speed condition. To illustrate this, control surface travel and corresponding stick force versus the off-speed condition is shown in figure 17 for the simulated SST and the SJT. Notice that at 20 knots below trim speed this SST control system required only 1.0 pound of force (over the 2.5 lb breakout force) compared to 16 pounds for the SJT. Thus the low static longitudinal stability and the low stick force gradient of the SST gave the impression of neutral static stability. The low static stability is the major contributor to this situation. For example, if the stick force gradient of the SJT had been utilized for the SST, the required trim force (disregarding breakout) would have been increased to about 2.5 pounds for the same 20-knot speed increment. Present air regulations regarding static longitudinal stability require that the average gradient of the stable slope of the stick force versus speed curve may not be less than 1 pound for each 6 knots (ref. 16, par. 25.173(c)). In order to meet this requirement, some tailoring of the stick-force-versus-speed characteristics would be required.

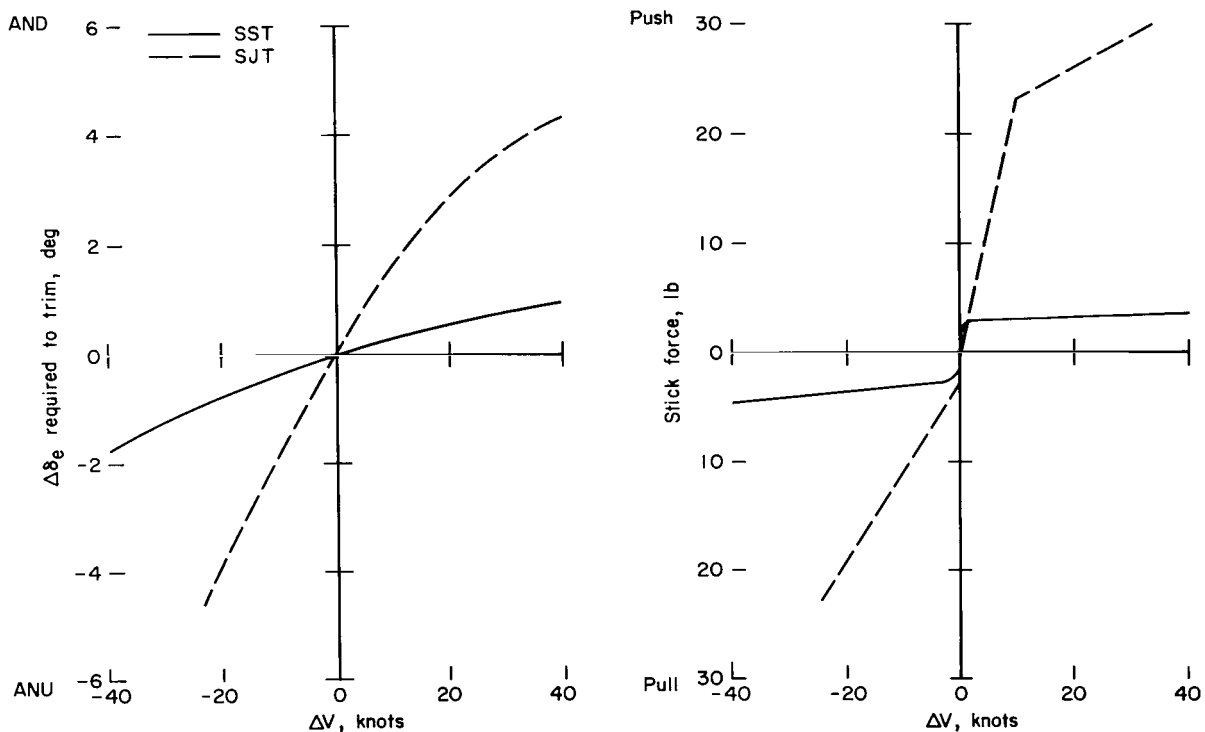


Figure 17.- Static longitudinal stability of simulated SST and reference subsonic jet transport; constant thrust. SST:  $W = 450,000$  lb, forward c.g. (s.m. = 0.039  $\bar{c}$ ),  $V_{trim} = 180$  knots. SJT:  $W = 300,000$  lb, midrange c.g. (s.m. = 0.21  $\bar{c}$ ),  $V_{trim} = 163$  knots.

Time histories of the dynamic response to an elevator step and doublet are presented in figure 18 for the delta SST and the reference subsonic jet transport. Among the SST's characteristics clearly shown are (1) effect of

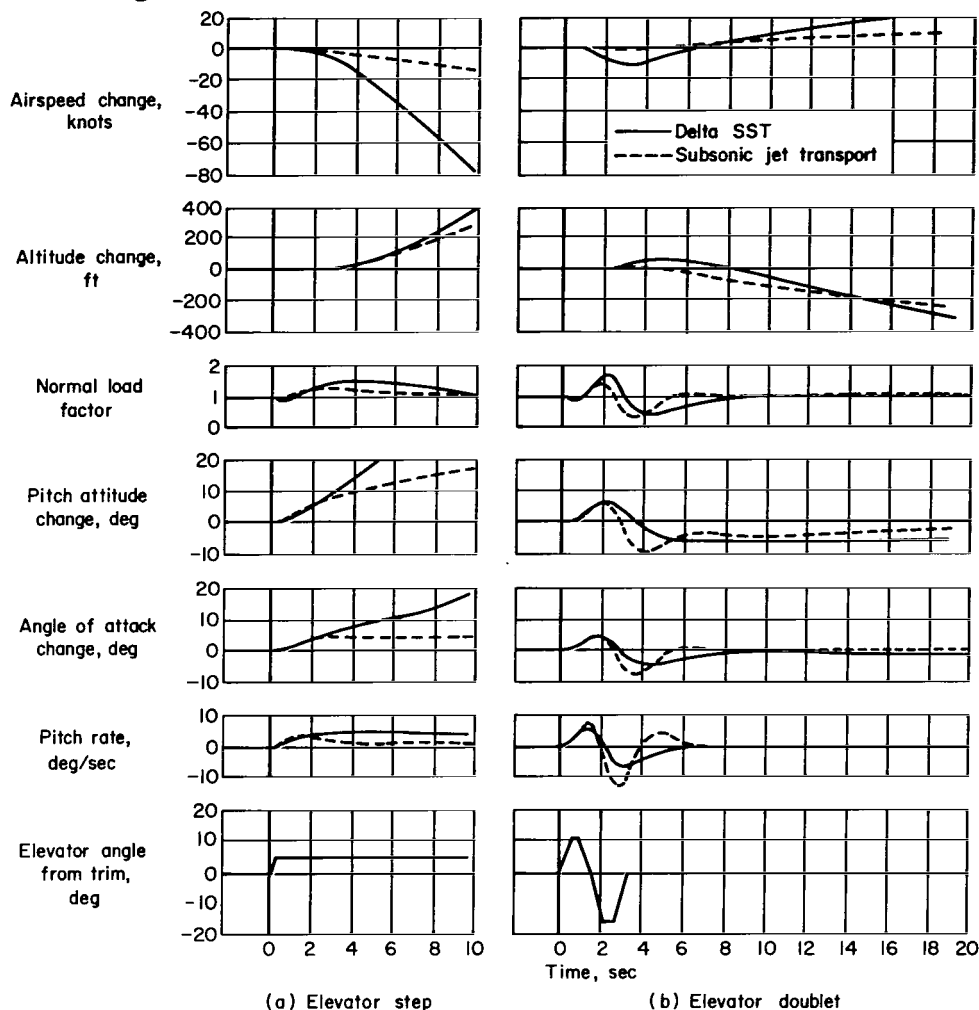


Figure 18.- Longitudinal dynamic response to control perturbations. Gross weight: SST 450,000 lb, SJT 300,000 lb; c.g. position: SST 2-percent static margin, SJT midrange; initial airspeed: SST 180 knots, SJT 163 knots.

the low static stability - in responding to the step input, the subsonic jet had assumed the new  $\alpha$  within about 2 seconds while the  $\alpha$  of the SST was still diverging 10 seconds following the same input; (2) greater sensitivity of airspeed to perturbations - shown in both responses; (3) lift loss due to elevator - nearly 1 second was required to begin developing a positive incremental load factor; and (4) higher damping and sluggishness - best illustrated in the response to the doublet.

Relationship of pitch attitude to airspeed.- During the initial climb of the delta SST at constant T/W, conventional relationships between steady-state airspeed and pitch attitude are somewhat modified, so that inadvertent speed changes are not reflected by pitch attitude changes. (Speed changes still involve conventional transitional variations of attitude.) Figure 19

presents the contributing elements to this characteristic. Plotted against speed are steady-state climb angle, angle of attack, and pitch attitude for the subsonic jet transport and the delta SST, both in the maximum-thrust

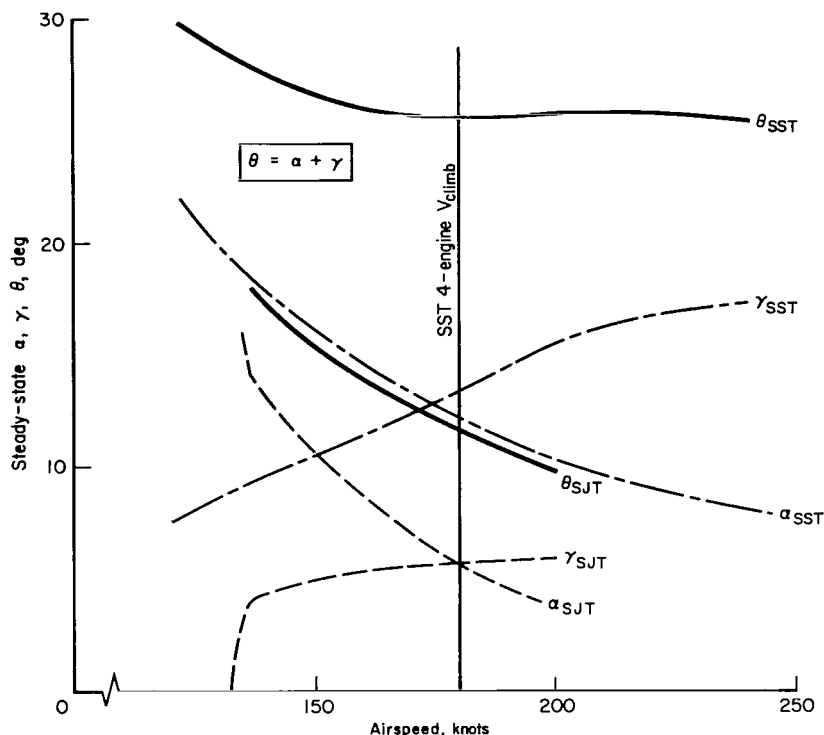


Figure 19.- Comparisons of steady-state pitch attitude and components ( $\alpha$  and  $\gamma$ ) versus speed for a subsonic jet transport and the simulated supersonic transport. Maximum thrust; gross weights: SST 450,000 lb, SJT 300,000 lb; SJT flaps  $15^\circ$ .

maximum-gross-weight condition. The large variation of induced drag with speed results in a steeper slope of the  $\gamma$  component, just offsetting the slope of  $\alpha$  for the delta SST simulated, with the result that pitch attitude remains constant over a wide range of airspeeds, and a single attitude does not define a single speed. With the subsonic jet, on the other hand, if the pilot holds a discrete pitch attitude, he establishes a unique airspeed.

Because of its unusual nature, such a characteristic should be pointed out in the training program for pilots transitioning into aircraft which exhibit it within the flight envelope. During the simulator runs, all pilots used airspeed and vertical velocity information in conjunction with the attitude indicator, and encountered no difficulty from the steady state  $\theta$  vs.  $V$  characteristic.

This characteristic could possibly prove advantageous in accelerated flight. It provides the pilot with a reference pitch attitude independent of airspeed. In addition, it appears feasible that the pilot might utilize the  $\theta$  vs.  $V$  characteristic of the delta SST to establish and maintain a desired

longitudinal acceleration (e.g., in an accelerating climb). If the flight path angle of any aircraft is varied (within the range normally encountered by transport airplanes) from that required for steady-state flight, the gravity component along the flight path will initially accelerate or decelerate the airplane at about 0.33 knot/sec-deg. For example, if the delta-SST pilot wishes to increase speed at a steady 1 knot/sec, he simply pitches the airplane  $-3^\circ$  (from the steady-state pitch attitude) and maintains this attitude until the desired speed is reached, then returns pitch attitude to the steady-state value. This maneuver in the reference SJT would cause an initial acceleration of 1 knot/sec, with acceleration "bleeding off," returning to zero as speed approaches the steady-state value corresponding to the decreased pitch attitude. Thus, the constant  $\theta$  vs.  $V$  characteristic could possibly facilitate speed adjustments, but whether this offsets the advantages provided by the speed-stabilizing tendency of the SJT remains to be proven.

Thrust-lever sensitivity.— Pilots stated that pitch attitude was quite sensitive to thrust-lever position. Since the thrust-lever travel was the same as for the SJT, and the SST has twice the available  $T/W$ , these comments were expected. It was not considered to be a problem. Figure 20 illustrates this sensitivity and presents pitch attitude and climb performance (at a constant climb speed) versus thrust setting. For example, a 20-percent thrust change results in a steady-state pitch attitude change of  $4.7^\circ$  for the SST, and only  $2.2^\circ$  for the SJT.

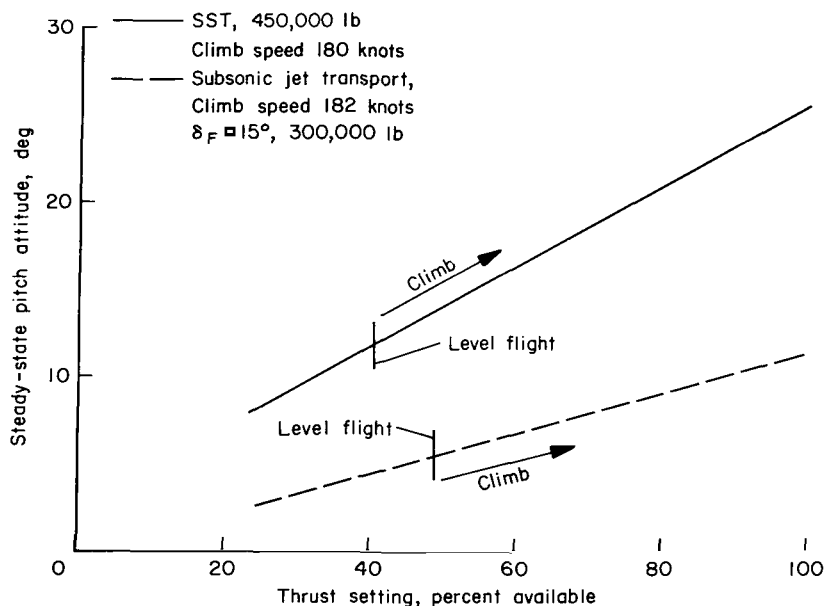


Figure 20.— Sensitivity of pitch attitude to thrust setting.

Additional information is provided by this figure regarding climb performance following an engine failure. With one engine out (75 percent available thrust on the figure), the SST still can maintain a  $7.9^\circ$  climb angle, while the SJT can maintain only a  $2.8^\circ$  climb angle.



## Lateral-Directional Characteristics

The possibility of engine failure during takeoff and the effects of the accompanying asymmetry necessitate consideration of the lateral-directional characteristics of the airplane. Therefore a brief description and evaluation is presented.

The derivatives estimated for the particular SST design simulated are listed in appendix A. The value of the yaw-damping derivative  $C_{n_r}$  - main contributor to damping of the Dutch roll oscillatory mode and also important to the spiral mode (ref. 21) - is significantly larger than for the SJT. (It is reasonable to compare the dimensionless derivatives for  $C_{n_r}$  because the dimensionalizing ratio  $Sb^2/I_z$  is similar for the two airplanes.) In addition, the derivative  $C_{n_p}$  - the change in yawing moment with varying roll rate - is fairly important in Dutch roll damping. Positive values of  $C_{n_p}$ , predicted for the double delta SST and used in this program, are to be desired; however, this quantity is negative for the SJT and most airframe configurations.

These estimates provided SST Dutch roll characteristics which were better than those of the SJT. The lateral-directional modes of motion for the unaugmented delta SST were well damped and exhibited no tendency to sustain a Dutch roll. Figure 21 shows the dynamic response to rudder and aileron pulses. The period of oscillation was about 7.5 seconds, about the same as exhibited by the SJT, and damped to one-half amplitude in 3.3 seconds. The

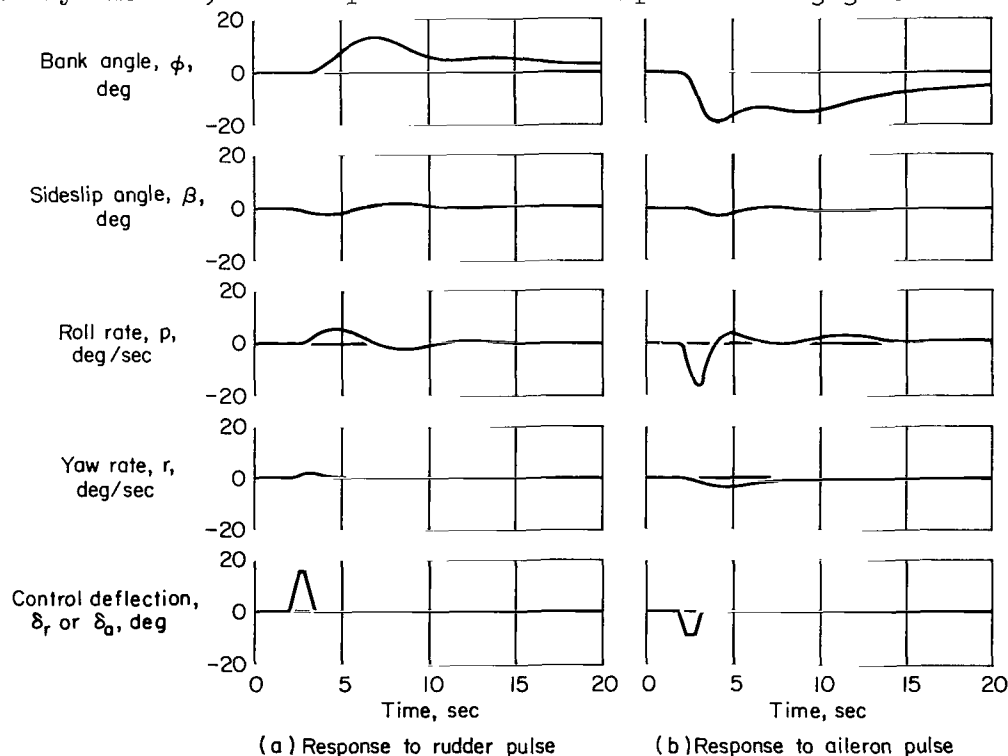


Figure 21.- Lateral-directional dynamic response of the unaugmented delta SST. Gross weight: 450,000 lb; airspeed 180 knots; gear retracted.

ratio of the bank-angle-to-sideslip-angle envelope  $|\phi|/|\beta|$  was about 2.5. Figure 22 compares the Dutch roll parameters,  $1/C_{1/2}$  and  $|\phi|/|v_e|$ , of the SST with those of the reference SJT, indicating the greater damping of the SST. (Military requirements, ref. 22, are also shown in the figure.)

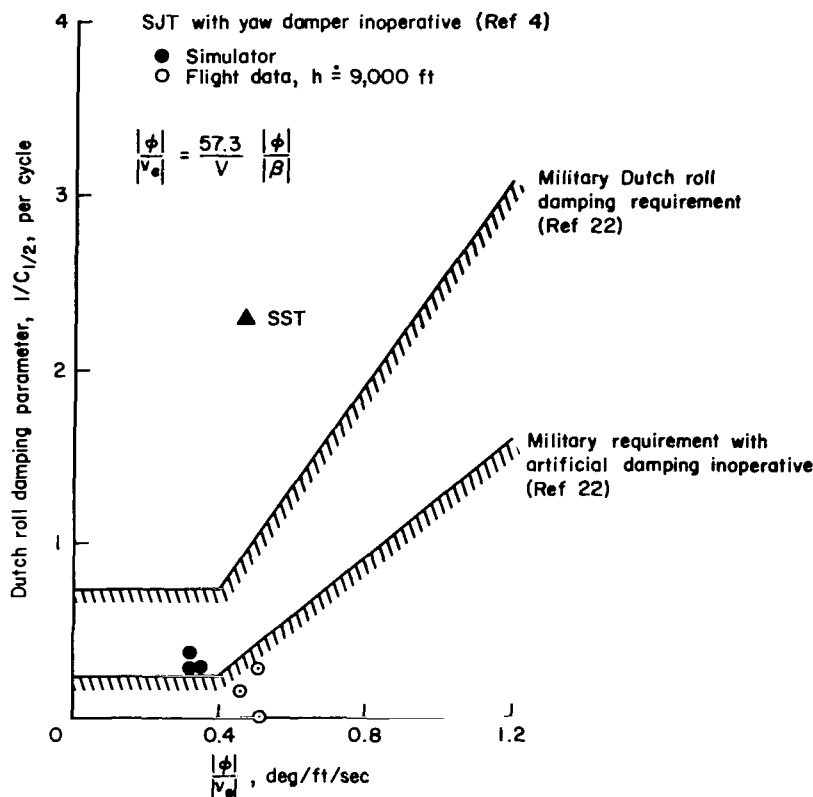


Figure 22.- Comparison of Dutch roll parameters of simulated SST and reference SJT during takeoff.

Lateral control power was good and the aircraft was responsive in roll. Turn entries required only slight use of the rudder into the turn for coordination. Adverse yaw was observable in the sideslip indicator but not apparent from the compass; this can be seen by comparison of the sideslip and yaw rate traces of figure 21(b). At the climb  $C_L$ , rudder was sufficient to generate approximately  $15^\circ$  of sideslip, requiring 50 to 60 percent of available aileron to maintain wings level.

Although not used for the majority of the tests, adding simple roll-rate and yaw-rate dampers made the lateral-directional oscillations critically damped - yet good response was retained.

## RESULTS AND DISCUSSION OF CERTIFICATION TASKS

The responses of the airplane and pilot-airplane loop during specific flight certification tasks are discussed. These tasks included three-engine takeoffs, the determination of minimum unstick speed, out-of-trim takeoffs, and the determination of air and ground minimum control speeds.

### Three-Engine Takeoffs

For investigation of the effect of engine failure during takeoff the pilots were exposed to engine failures at various points throughout the take-off run and climbout; some were surprise cuts while others occurred during scheduled three-engine tests. Nearly all engine cuts were on an outboard engine, but the pilot did not know from which side to expect the failure. Many of the three-engine takeoffs were made without the visual scene, that is, under simulated instrument conditions. Pilots were told to abort the takeoffs if an engine failed below  $V_1$  (equal to  $V_R$  during these tests) and to continue the takeoff if it failed above  $V_1$ . This discussion pertains to those takeoffs that were continued following the failure.

— No stability augmentation  
 ---- Roll damper operative ( $\delta_{ard} = -1.25 \dot{\phi}$ )

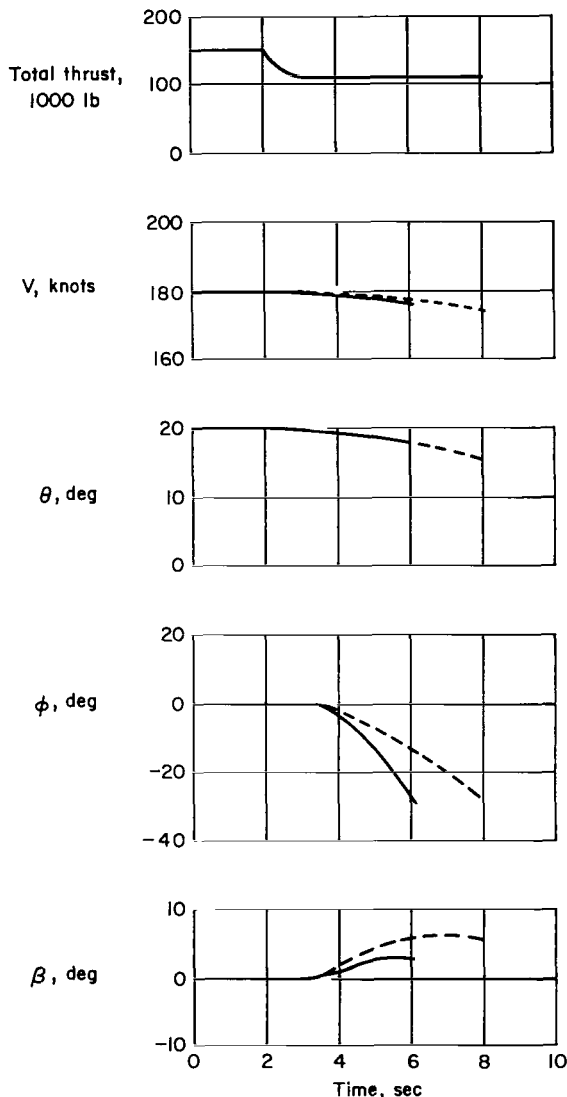


Figure 23.- Uncontrolled response of simulated SST to outboard engine failure. Gross weight 450,000 lb; noise-abatement thrust; engine time constant 0.4 second.

Airplane response to engine failure.- With the test SST, engine failures were accompanied by a significant rolling response (when not restrained by the ground). This was primarily due to the gross difference between the rolling and yawing moments of inertia; thus  $L_\beta/N_\beta$  (the ratio of rolling-acceleration-due-to-sideslip to yawing-acceleration-due-to-sideslip) was relatively high, although  $C_{l_\beta}/C_{n_\beta}$  was lower than for the SJT. Consequently, the sideslip following an engine failure generated substantial rolling motions.

Figure 23 demonstrates the uncontrolled responses of the airplane following failure of the outboard engine during a noise-abatement climb with the roll rate damper ( $\delta_{ard} = -1.25 \dot{\phi}$ ) both operative and inoperative. No artificial damping in yaw was utilized. Without corrective control inputs, bank angle reached  $30^\circ$  in slightly over 4 seconds for the unaugmented case. Sideslip angle peaked at  $6^\circ$  with roll augmentation and  $3^\circ$  without roll augmentation, while airspeed began to decrease slowly, dropping 5 knots in 6 seconds. The engine time constant of 0.4 second for these runs may be less than will exist on

the actual airplane, which makes the results somewhat conservative; that is, the response would be less severe on the actual airplane.

Controlled takeoffs after engine failure.- A series of 15 piloted noise-abatement takeoffs were made without the visual scene in which an outboard engine was failed approximately 1 second after  $V_R$  ( $V_R = 152$  knots) was reached. After the failure was recognized, additional thrust was applied on the remaining three engines (bringing the thrust up to 43,000 lb/engine) and the takeoff continued. The roll-rate damper was operative during these runs.

In general, the three-engine takeoffs were controlled satisfactorily, despite long recognition times. The time from engine failure to corrective rudder input varied from 0.8 to 5.8 seconds. The wide range is attributed to the absence of motion or external visual cues. Two of the pilots had applied corrective action within 0.8 to 3.1 seconds while a third pilot, apparently not using the same instrument information in detecting the failure, required approximately 4 seconds, with one value as high as 5.8 seconds. Maximum side-slip angles ranged from  $3^\circ$  to  $5.5^\circ$  and occurred 1.5 to 7 seconds after lift-off. The roll rate developed during lift-off was readily corrected with pilot input. Peak bank angles were less than  $8^\circ$  and occurred 2 to 7.5 seconds after lift-off. Approximately 70 percent of the available rudder deflection<sup>1</sup> and 40 percent of the available aileron (elevon) deflection were used in maintaining control.

Lift-off speed was generally about 4 to 5 knots below the normal  $V_{LOF}$  of 169 knots. Median  $V_{35}$  was 173 knots, ranging from 165 to 178 knots; corresponding times from lift-off to the 35-foot height were 3 to 13 seconds, with a median of 9 seconds. A positive climb rate was maintained following lift-off, with the aircraft reaching a height of about 200 feet over the end of the 10,000-foot runway. Once climb speed was reached, deviations in air-speed were within  $\pm 6$  knots, better for some of the pilots than their four-engine speed control, presumably because of their intense concentration during this task. Pilots reported no particular problem in holding heading throughout the climb.

The primary conclusion is that even with the long recognition times, the maneuver was accomplished successfully, partially because of the good lateral-directional characteristics. Speed control, per se, was not a serious problem although close attention was required for acceleration to the desired climb speed at low T/W. The task of accelerating to climb speed would probably have been facilitated by a larger and more easily read pitch attitude indicator.

Engine failures during the climb were quite noticeable because of the attendant rolling motion, but lateral control response was good and the airplane was easy to control once the roll was arrested.

---

<sup>1</sup>Rudder travel was limited to  $25^\circ$  (compared to  $30^\circ$  for the majority of the tests) and  $C_{n\delta_r}$  was reduced for this series of 15 takeoffs. See appendix A.

Engine-out crosswind takeoffs.- The effect of crosswind in combination with engine failure during the takeoff was investigated and, again, the possibility of nacelle strike was indicated for this type of aircraft. Figure 24

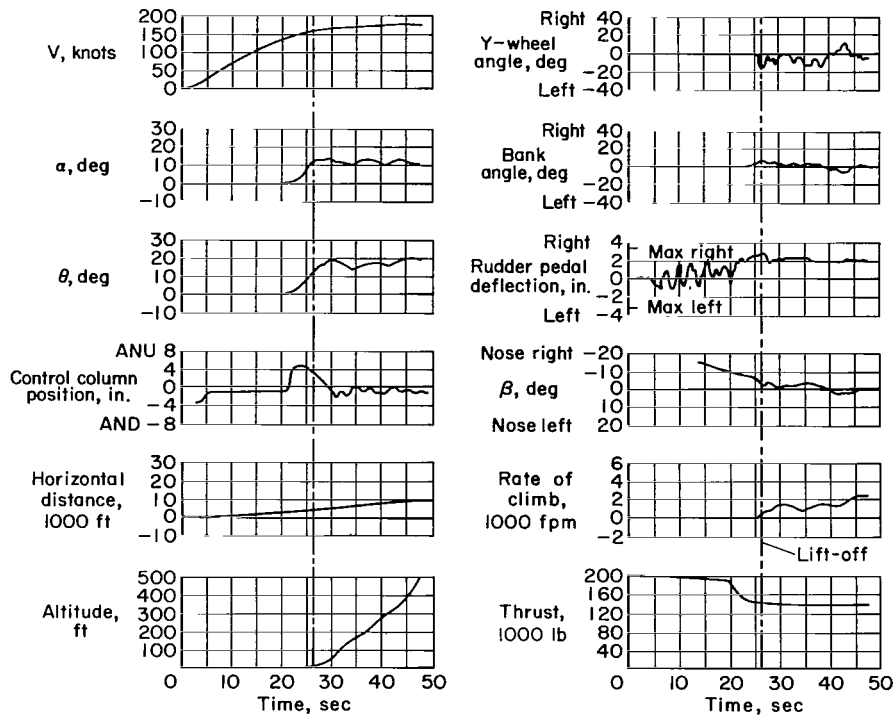


Figure 24.- Maximum thrust takeoff with left outboard engine failure; 30-knot crosswind from left.

presents a time history for a maximum thrust takeoff with a left outboard engine failure occurring at  $V_R$ . The crosswind component was from the left at 30 knots, stability augmentation was off, and rudder-pedal nose-wheel steering was operative. Engine response was represented by a 2.0 second first-order time constant.

During this run, bank angle reached  $6^\circ$  at lift-off, causing a nacelle strike, even though lift-off pitch attitude was  $13^\circ$ . (The simulator program did not provide rolling or yawing moments due to nacelle strikes.) The rolling tendency during the lift-off was generated primarily by the dihedral effect in response to the aerodynamic sideslip induced by the crosswind.

Summary of engine-failure studies.- In summary, engine failures during takeoff (after  $V_1$ ) caused no undue difficulty. Recovery following engine failure was easier in the SST than in the SJT. This can be attributed to the good lateral-directional characteristics and to good three-engine performance.

#### Determination of Minimum Unstick Speed, $V_{MU}$

The minimum unstick speed  $V_{MU}$  is defined as the speed at and above which the airplane can be made to lift off the ground and continue the takeoff without displaying any hazardous characteristics.

A decrease in  $C_{L_{max}}$  near the ground has been shown for swept-wing aircraft of moderate to high aspect ratio utilizing flap devices (refs. 23 and 24). This proximity to the stall or the critical acceleration margin ( $T - D$ ) at high lift-off attitudes or both necessitated the requirement for demonstrating  $V_{MU}$  on the subsonic jet transport. Flight test determination of  $V_{MU}$  involves a maneuver that is often hazardous and difficult to fly.

The delta SST is limited by its geometry to takeoff attitudes below those which would yield  $C_{L_{max}}$  or a drag-limiting condition (with normal thrust levels). Demonstration of  $V_{MU}$  does not have the significance for geometry-limited airplanes that it had for drag-limited airplanes and is being re-evaluated as a certification requirement for geometry-limited supersonic transports.

However, this maneuver was examined on the simulator and several items of interest were noted. These were with regard to the effect of combinations of low thrust and low lift-off speed and the loss of lift due to excessive elevator deflection.

$V_{MU}$  test procedure.- Minimum unstick speed was determined and the accompanying flight characteristics were evaluated for one-engine-inoperative and all-engines-operating conditions. Static thrust settings ranged from 30,000 to 50,000 pounds per engine. A forward c.g. providing a static margin of 5-percent  $\bar{c}$  was used for these tests.

The procedure for determining  $V_{MU}$  was to apply full nose-up elevator early in the takeoff acceleration run (at approximately 100 knots), and to maintain this control input so that the desired lift-off pitch attitude could be attained at the lowest possible speed. Following lift-off, the airplane climb out of ground effect was at the lowest practicable speed. Gear retraction was initiated approximately 4 seconds following lift-off. An outboard engine failed between 120 and 130 knots for the three-engine  $V_{MU}$  test. Rudder-pedal nose-wheel steering was operative.

General  $V_{MU}$  characteristics.- Figure 25 shows a time history of a maximum-thrust four-engine  $V_{MU}$  test. An artificial test condition of maintaining full back column until lift-off was used in many of the simulator  $V_{MU}$  runs, thus allowing the nacelles to contact the runway. Nose-wheel lift-off started generally at about 126 knots, regardless of thrust setting, demonstrating adequate longitudinal control power. Pitch rate at the instant of nacelle strike was  $5.5^{\circ}$  to  $7.0^{\circ}/\text{sec}$ . The pitch dynamics of the SST made it difficult to establish and maintain a desired ground clearance (e.g., 1 ft) until lift-off. Attempts to stop the pitch rate before nacelle strike generally arrested rotation prematurely and delayed lift-off.

Both three- and four-engine tests yielded lift-off speeds from 148 to 152 knots. However, most lift-offs at 148 knots were momentary with final lift-off at 152 knots. Thus  $V_{MU}$  was considered to about 152 knots. During the  $V_{MU}$  tests at reduced thrust levels, the nacelles dragged along the runway until the airplane accelerated to lift-off speed, while at the maximum

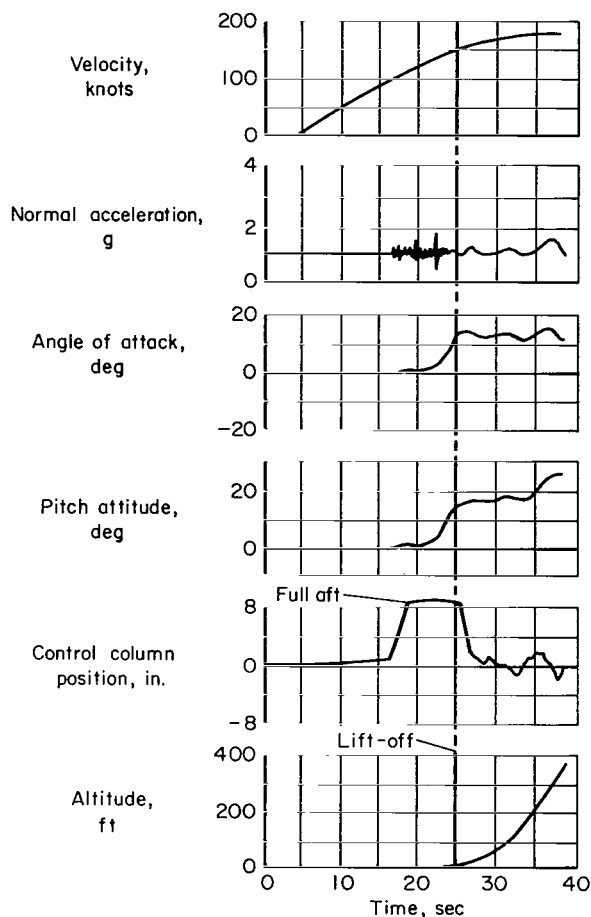


Figure 25.- Maximum-thrust four-engine  $V_{MU}$  test.

T/W condition, nacelle strike was nearly simultaneous with lift-off. At maximum and noise-abatement thrust levels, handling characteristics of the delta SST in the  $V_{MU}$  maneuver were considered better than those of the simulated subsonic jet transport, again largely because of the better lateral-directional characteristics, greater thrust margin, and absence of stall proximity.

Effect of speed abuse on low-thrust takeoffs.- Minimum-unstick-speed tests at low thrust levels focused attention on the performance sensitivity of the SST to lift-off speed abuse when thrust levels are marginal. Anticipated T/W values for the SST will likely provide climb gradients in excess of present requirements; however, certain combinations of conditions might result in marginal performance for this aircraft.

Several items contribute to the SST's performance sensitivity, primarily (1) greater rate of degradation in climb gradient with reduced speed (greater induced drag) than exhibited by the SJT, and (2) large ground plane influence on lift and drag.

These points appear more meaningful when one considers the hypothetical example represented in figure 26, in which the assumed performance just satisfies the existing first segment<sup>2</sup> gradient requirement of 0.5 percent at  $V_{LOF}$  (ref. 16, par. 25.121(a)). Delta-wing aerodynamics from several sources indicate that the slope of climb gradient versus speed is on the order of +0.2 percent per knot in this speed region. In other words, if for some reason the airplane were to lift off early, or decelerate after lift-off, a speed 3 knots less than the criteria-satisfying  $V_{LOF}$  would yield a negative climb gradient out of ground effect. The subsonic jet, on the other hand, has a margin of 7 knots or greater.

The influence of full ground effect in this speed region is to add an incremental gradient of about 0.06 to 0.07 onto the climb performance of the SST. (This compares with an incremental climb gradient increase due to full ground effect of about 0.05 shown in reference 24 for the slotted-wing DC-8 subsonic jet transport with 25° flaps and at  $V_{MU}$ .) Notice that for lift-off

<sup>2</sup>First segment identifies flight condition: critical engine (outboard) inoperative, gear extended, out of ground effect, speed equal to  $V_{LOF}$ .

Conditions:

1.  $V_{LOF}(3\text{-engine}) = 1.05 V_{MU}$  (Par 25.107 (e) ref 16)
2. Gradient at  $V_{LOF} = 0.5$  percent (Par 25.121 (a) ref 16)

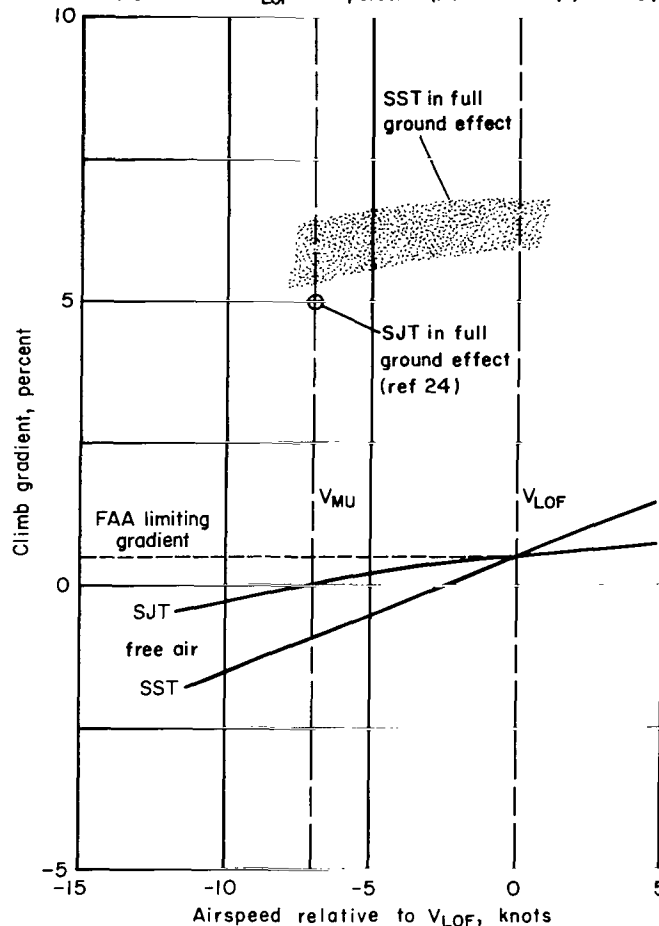


Figure 26.- Effect of low takeoff speed on minimum-thrust climb performance.

at the  $V_{MU}$  speed, climb gradient is positive, but if the airplane is flown out of ground effect without accelerating, level flight cannot be sustained. Consequently, the delta SST must be accelerated while in ground effect whereas the SJT could manage to maintain level flight out of ground effect. On the other hand, at  $V_{MU}$  the reference SJT was only a few knots above the in-ground-effect stall speed, whereas the characteristics of the delta-planform airplane eliminate this hazard.

This discussion suggests that perhaps the first-segment climb gradient criterion (which was satisfactory for the swept-wing transports) may require some modification before it can be applied to delta-winged transport aircraft.

Effect of lift loss due to elevator deflection.- Loss of lift due to elevator deflection significantly affects the lift available for takeoff of the tailless delta airplane. This was especially evident for the somewhat artificial situation used in many of the simulator runs where full back column



was held and the nacelles were allowed to drag until lift-off occurred. Variations in resultant lift-off speed for departures from the test values of  $C_{L\delta_e}$  (lift decrement per unit elevator deflection) were examined for this condition. A simple statics computation produced figure 27 which demonstrates this effect. Plotted versus speed are the vertical forces: aircraft weight, thrust component ( $T \sin \alpha$ ), lift due to  $\alpha$ , lift decrement due to full elevator deflection, and the total of these forces. The speed at which the total-vertical-force curve passes through zero can be interpreted as the minimum unstick speed. Plotted in the inset is the resultant  $V_{MU}$  versus the corresponding value of  $C_{L\delta_e}$ . This plot verifies the  $V_{MU}$  speed of 152 knots for the basic simulator  $C_{L\delta_e}$ . It also points out that if a  $C_{L\delta_e}$  50 percent

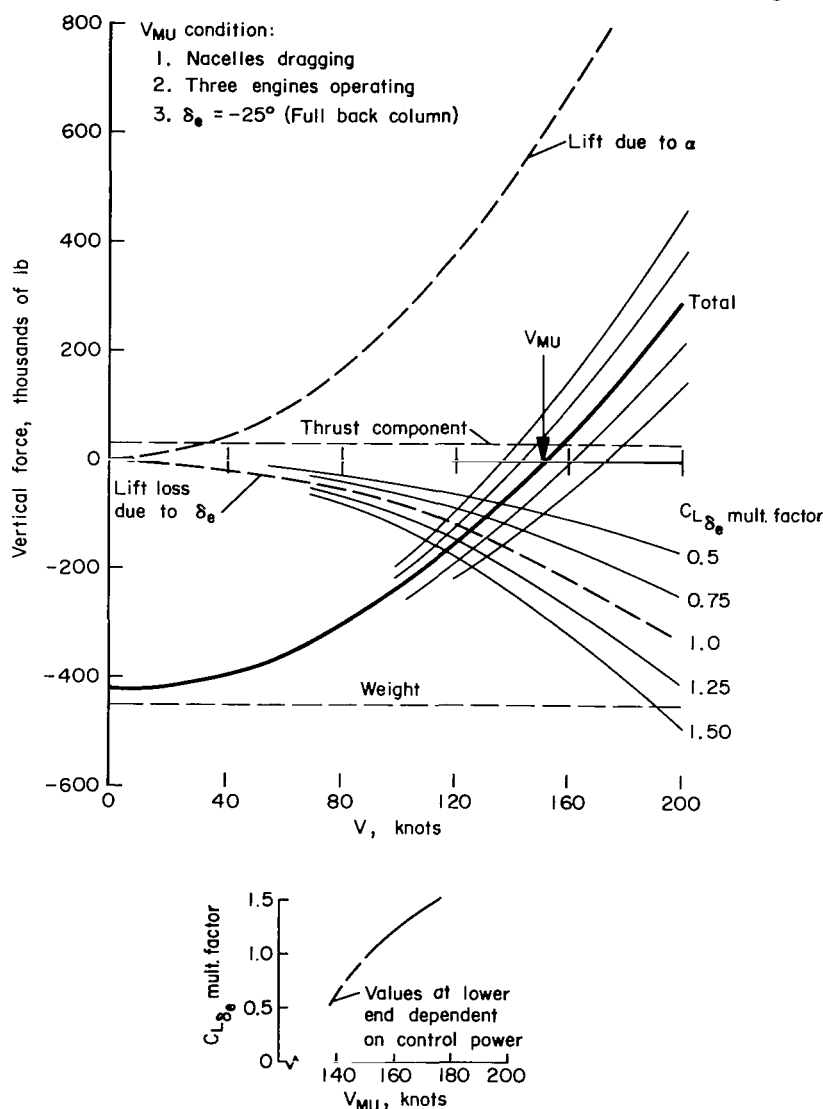


Figure 27.- Effect of  $C_{L\delta_e}$  on  $V_{MU}$  speed for a tailless delta SST.

greater than that used in the simulator runs were used,  $V_{MU}$  would be delayed until 175 knots or until some of the back stick force were relaxed.

This means that if  $V_{MU}$  were determined for this type of aircraft by rotating to the geometry limit, the resultant speeds would display considerable scatter dependent upon the amount of excess elevator deflection being applied. This effect was verified by simulator runs in which  $C_{L\delta_e}$  was increased by 50 percent. The lift-off speeds ranged from 150 to 175 knots.

#### Ground Minimum Control Speed

Following an outboard engine failure, the minimum speed at which the maximum lateral deviation from the runway center line can still be held to 15 feet<sup>3</sup> was termed minimum ground control speed  $V_{MCG}$ . This was determined by plotting the results of a number of takeoff ground runs in which engine failure occurred at successively lower speeds. The pilot applied full corrective rudder as soon as he recognized the engine failure. Maximum takeoff thrust and aft c.g. were used for the majority of the runs.

Simulator results, nose-wheel steering inoperative. - The simulator results are shown in figure 28 where the maximum unavoidable deviation from runway center line is plotted against the corresponding speed at which the

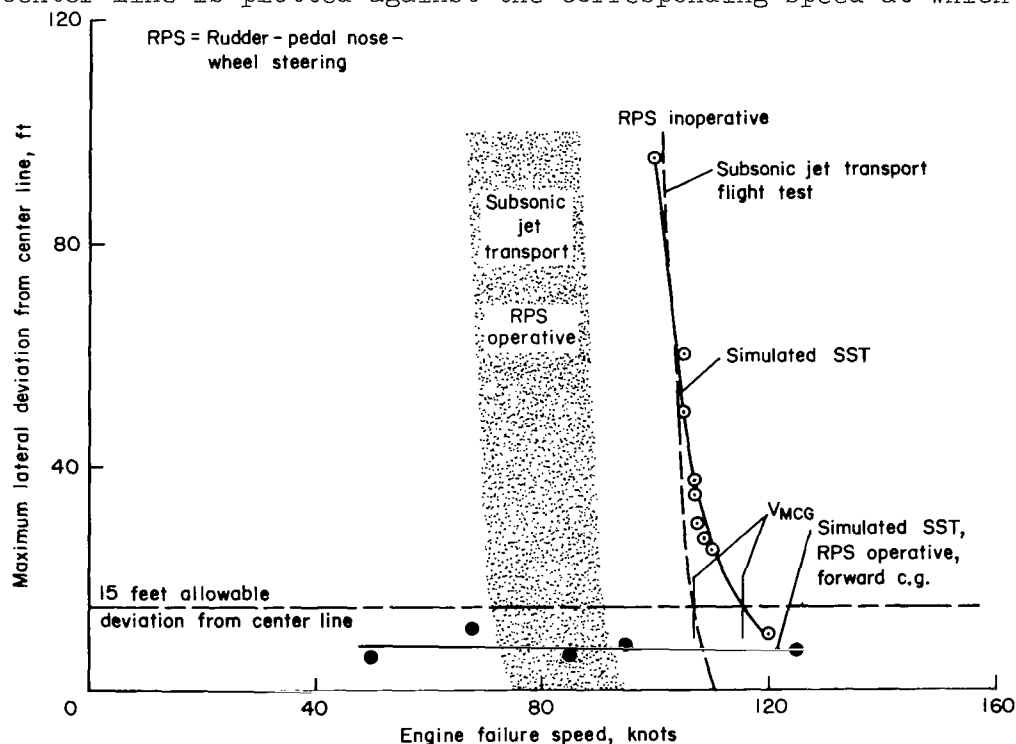


Figure 28.- Determination of ground minimum control speed. Asymmetric thrust: SST 50,000 lb; SJT 14,700 lb. Gross weight: SST 450,000 lb; SJT 180,000 lb. Aft c.g. except as noted.

<sup>3</sup>A value of 15 feet was used during the certification tests of the reference SJT to be conservative. The FAA and the military often allow 25 feet.

engine failed. With 50,000 pounds asymmetric thrust and the rudder-pedal nose-wheel steering inoperative, the  $V_{MCG}$  of the simulated SST was 115 knots - of the same order as the reference subsonic jet transport (107 knots) at maximum takeoff thrust.

Effect of high  $T/W$  on  $V_{MCG}$ . - The high longitudinal acceleration of the SST makes it more "forgiving" than the SJT of continued takeoffs following engine failure a few knots below  $V_{MCG}$  (continuing the takeoff is not being advocated here). This was noted by the pilots who had participated in certification of the SJT. When an engine on the subsonic jet failed at 10 knots below  $V_{MCG}$ , the airplane traveled off the edge of the runway (greater than 100 ft deviation) unless thrust was reduced on the opposing engines. In the case of the SST, a failure 10 knots below its  $V_{MCG}$  resulted in less than 50 feet of lateral deviation. This lesser deviation resulted from the more rapid attainment of speeds where directional control power was adequate, because of the higher  $T/W$  of the SST. For example, at maximum takeoff thrust, SST acceleration following engine failure was about 6 knots/sec, as compared to about 3.5 knots/sec for the reference subsonic jet transport at the test condition shown.

This beneficial effect of high  $T/W$  was verified on the simulated SST by repeating a series of  $V_{MCG}$  runs with thrust on the inboard engines reduced to 10,000 pounds each. The acceleration following engine failure was then more representative of a SJT, yet the thrust asymmetry condition of the SST was retained. The resultant  $V_{MCG}$  was nearly equal to that determined in the previous tests, but the slope of the curve was much steeper and comparable to that shown for the SJT flight results.

Effect of nose-wheel steering on  $V_{MCG}$ . - Flight tests of the SJT demonstrated that a substantial reduction in  $V_{MCG}$  could be realized with nose-wheel rudder-pedal steering (RPS). With RPS operative and dry runway conditions, the reference SJT experienced a reduction in  $V_{MCG}$  of 15 to 35 knots, depending upon nose-gear load. There are factors, however, which reduce the effectiveness of RPS (e.g., fuselage flexibility, wet or icy runway, etc.). With a structure like that of the SST, fuselage flexibility (not included in this simulation) could cause fluctuations in nose-gear loading that would reduce the benefits to be derived from nose-wheel steering.

The SST configuration tested on the simulator incorporated no high-lift devices and the wing was at a slightly negative angle of attack during the ground run. This increased the loading on the nose gear for improved directional control with RPS operative and on the main gear for more effective braking.

The only simulator data points acquired for the SST with RPS operative were with a heavyweight forward c.g. condition - and therefore, represent a rather optimistic limit. This condition resulted in a heavily-loaded nose gear which thus could generate a turning moment through RPS large enough to counter the thrust asymmetry. (Maximum side-force coefficient was assumed to be 0.5. See ref. 4 for details regarding simulator programming.) Therefore

engine failures at speeds as low as 50 knots were controlled with less than 10 feet of lateral deviation. Rough calculations indicate that at lighter weights or with aft c.g. loading, the deviations would be greater.

#### Air Minimum Control Speed

Air minimum control speed  $V_{MCA}$  was determined by gradually slowing the airplane until full rudder control was required to maintain a constant heading with an outboard engine inoperative and maximum thrust from the other outboard engine. Aileron control was used in holding a  $5^\circ$  bank angle to assist the rudder.

For the  $V_{MCA}$  tests, gross weight was reduced to 265,000 pounds and the c.g. was aft. Testing was conducted with landing gear retracted and extended; when the gear was retracted, the top panel of the three-panel rudder was inoperative in the assumed mechanization. Stability augmentation was off for all  $V_{MCA}$  runs.

$V_{MCA}$  test results. - Table IV presents the minimum control speed and corresponding parameters of interest for the landing gear retracted and extended cases.

TABLE IV.- AIR MINIMUM-CONTROL-SPEED TEST RESULTS

	Landing gear retracted (two-panel rudder)	Landing gear extended (three-panel rudder)
$V_{MCA}$ , knots	108	104
$\delta_a$ required, percent of available	84	57
Angle of attack, deg	16-17	16-17
Sideslip angle, deg	10	6
Asymmetric thrust, lb	48,300	48,400

For comparison, the reference subsonic jet transport at maximum thrust exhibited a  $V_{MCA}$  of 117 knots (asymmetric thrust, 14,500 lb). The results show that, even with maximum thrust, simulated SST engine-out conditions were controllable to lower airspeeds than the SJT.

In addition, air minimum control speeds were more easily determined with the test SST than with the simulated subsonic jet. This was attributed to the following: (1) the airplane had good lateral-directional characteristics, (2) tests were not in a region of impending stall where the pilot's ability to maintain control is degraded due to buffeting, and (3) the lateral control system had no abrupt changes in linearity due to spoiler assist, etc.

The speed stability problem, discussed earlier in relation to normal climbout procedures, was not significant in this tightly-controlled test maneuver, despite flight at airspeeds within the stick-shaker region (angles of attack greater than  $17-1/2^\circ$ ).

### Out-of-Trim Takeoffs

Much of the difficulty encountered during mistrim takeoffs is due to the surprise of the situation and to the uncertainty as to the source of the problem. The pilot suddenly discovers the airplane is not responding as expected. The longitudinal trim mechanization chosen for the simulated SST warned the pilot of a mistrim condition by the unnatural control column position. With this system, actuating trim drove the control column, as well as the elevator (elevon) surfaces, to a new position. In comparison, the control column position of the SJT is not changed by the trim system which repositions the horizontal stabilizer. Because both the trim and column-actuated control systems used the same control surfaces, varying trim setting did not change the maximum control power available for the rotation maneuver of the simulated SST (assuming fixed surface travel limits) as it does on the subsonic jets with variable-incidence horizontal stabilizers. These appear to be two favorable factors in reducing the probability for mistrim takeoff incidents.

Simulator takeoffs were made with large amounts of airplane nose-up and airplane nose-down mistrim. Elevator deflections corresponding to the mistrim conditions were  $-14.5^\circ$  (ANU) and  $8.6^\circ$  (AND).

Takeoff with full nose-down mistrim. - Full nose-down mistrim at forward c.g. generally resulted in a slower rotation, slightly delayed lift-off, overshoot of the target climb speed, and pilot-induced oscillation in pitch attitude of  $\pm 2^\circ$  immediately after lift-off. This trim condition required an additional 15 pounds of pull force during rotation and climb.

Takeoff with full nose-up mistrim. - Full nose-up mistrim runs at aft c.g. were easily identified by the premature self-rotation at approximately 135 knots. The pilots arrested the rotation rate at  $6^\circ$  to  $7^\circ$  pitch attitude, then allowed rotation at the scheduled  $V_R$ , inadvertently allowing overrotation which caused an early lift-off. Due to the unnatural push forces required during the transition and climb, a pilot-induced oscillation resulted as the speed was worked up to the target value. Push force required at  $V_{climb}$  was approximately 25 pounds. This was with a force gradient of 3.5 pounds per inch - a low gradient by today's SJT standards.

Because the pilots were forewarned of the out-of-trim condition, this test was one of controlling the takeoff with abnormal control forces and provided no significant problems. Owing to the control system characteristics and the performance margin of the simulated SST, the hazards of an out-of-trim takeoff do not appear as great as with the SJT.

## PILOT ACCEPTANCE OF THE Y-SHAPED CONTROL WHEEL

Since a novel Y-shaped control wheel (fig. 2) was being considered for the SST, it was considered appropriate to evaluate such a control in this test program. Comparative evaluation was possible because a conventional control wheel was used for a number of simulator runs early in the program.

Basically, pilots did not feel that using the Y-shaped wheel compromised the evaluation of the aircraft characteristics. It did provide improved instrument visibility, but the manipulative convenience of the controller was questionable. Pilot opinions in this regard ranged from "acceptable" to "awkward," the latter stemming from tests requiring simultaneous use of large lateral and longitudinal inputs. Lateral inputs require that a side force be applied to the grip, as compared to the conventional control wheel movement. This lateral force proved to be fatiguing during prolonged periods of lateral input (e.g., minimum control-speed testing). Additional effort regarding the Y-wheel geometry, seat armrests, control force gradients and breakout, etc., might improve the pilot acceptance of this type of control arrangement.

## SUMMARY OF RESULTS

The following takeoff characteristics of a generalized double-delta planform SST are based upon the fixed-cockpit simulator study of the unaugmented airplane:

1. Several items of significance were noted with regard to the rotation maneuver.
  - (a) The pitch dynamics and low margin of ground clearance resulted in a high probability of nacelle or tail strikes for the configuration tested. Bank angles induced at lift-off by crosswind conditions aggravated this tendency. Three possible solutions, each with certain disadvantages, include: (1) slowed, more consistent rotations, (2) lengthening of the landing gear, and (3) higher lift-off speeds.
  - (b) The high longitudinal acceleration of the SST, especially if combined with a slow rotation, will require a large speed margin between  $V_R$  and the target lift-off speed, considerably greater than for the subsonic jet transport.
  - (c) In order to insure a safe rotation and lift-off with one-engine inoperative, high lift-off speeds may result when all engines are operating.
  - (d) Present airworthiness criteria requiring that  $V_R$  provide a  $V_{LOF}$  not less than 105 percent  $V_{MU}$  with one-engine inoperative nor less than 110 percent  $V_{MU}$  with all engines operating with

the airplane rotated at the maximum practicable rate may be unduly penalizing to the SST at high T/W.

2. Primarily because of the pitch dynamics and because it was aggravated by negative speed-thrust stability, the SST tended to wander in pitch attitude and in airspeed, thus required greater attention than the subsonic jet transport during constant speed climbout. The pilots considered these characteristics acceptable but unpleasant.

3. At the SST's high thrust-weight ratio, runway distance to clear a 35-foot obstacle ( $s_{35}$ ) was relatively insensitive to the speed at which rotation was initiated. Runway distance was considerably more sensitive to the target lift-off attitude than the subsonic jet transport, with increasingly higher attitudes (up to the geometry limit) reducing  $s_{35}$  and low attitudes significantly increasing the distance.

4. The estimated lateral-directional stability derivatives for the subject SST provided much improved Dutch-roll characteristics over those of the subsonic jet transports. This factor, in combination with the larger performance margin, made SST handling characteristics following engine failure generally better than those of the subsonic jets.

5. Minimum control speeds (ground and air) were of the same order as, or lower than, those for the reference subsonic jet transport. In addition, the high T/W (good longitudinal acceleration) of the SST makes it more "forgiving" than the SJT of continued takeoffs following engine failure a few knots below  $V_{MCG}$  (as established by current procedures).

Ames Research Center

National Aeronautics and Space Administration

Moffett Field, Calif., 94035, Aug. 24, 1967

720-04-00-05-00-21

## APPENDIX A

### LATERAL-DIRECTIONAL DERIVATIVES AS USED IN THE SIMULATOR INVESTIGATION

Derivatives are dimensionless, referred to body axes, and linearized for simplification of programming.

$C_{l\beta}$	$-0.030 - 0.515 \alpha$	$(\alpha \text{ in radians})$
$C_{n\beta}$	$0.100 + 0.103 \alpha$	
$C_{Y\beta}$	$-0.424 + 0.855 \alpha$	
$C_{l_r}$	$0.785 \alpha$	
$C_{n_r}$	$-0.400$	
$C_{l_p}$	$-0.139 - 0.690 \alpha$	
$C_{n_p}$	$0.040 + 0.545 \alpha$	
$C_{l_{\delta a}}$	$0.120$	
$C_{n_{\delta a}}$	$0.018$	
$C_{l_{\delta r}}$	$-0.0107$	
$C_{n_{\delta r}}$	$0.0745$	
$C_{Y_{\delta r}}$	$-0.0957$	

The data presented in the discussions of the uncontrolled response to out-board engine failure and the 15 noise-abatement engine-out takeoffs were obtained using a slightly different set of derivatives from those listed above. These were generally within  $\pm 15$  percent of the values shown above, with the exceptions of  $C_{l\beta}$  (27 percent greater),  $C_{n_r}$  (25 percent greater), and  $C_{n_{\delta r}}$  (24 percent less).



## REFERENCES

1. Tymczyszyn, Joseph J.; and Spiess, Paul C.: The Effects of Supersonic Transport Flight Characteristics on Performance Requirements. Paper 674 D, SAE and ASNE, April 1963.
2. Tymczyszyn, Joseph J.: Flying Characteristics of the Supersonic Transport. Paper presented to the International Federation of Airline Pilots Association (London, England), Nov. 1963.
3. Jackson, Charles T., Jr.; and Snyder, C. Thomas: A Simulator Study of Take-Off Characteristics of Proposed Supersonic Transports. Conference on Aircraft Operating Problems, NASA SP-83, 1965, pp. 149-157.
4. Jackson, Charles T., Jr.; and Snyder, C. Thomas: Validation of a Research Simulator for Investigating Jet Transport Handling Qualities and Airworthiness Criteria During Takeoff. NASA TN D-3565, 1966.
5. Bray, Richard S.: A Piloted Simulator Study of Longitudinal Handling Qualities of Supersonic Transports in the Landing Maneuver. NASA TN D-2251, 1964.
6. Cooper, George E.: The Use of Piloted Flight Simulators in Take-off and Landing Research. AGARD Rep. 430, Jan. 1963.
7. Spence, A.; and Lean, D.: Some Low-Speed Problems of High-Speed Aircraft. AGARD Rep. 357, April 1961.
8. Foss, R. L.; Magruder, W. M.; Litrownik, I.; and Wyrick, D. R.: Low-Speed Aerodynamic Characteristics of the Double-Delta Supersonic Transport. AIAA paper 64-591, 1964.
9. Goldsmith, H. A.: Stability and Control of Supersonic Aircraft at Low Speeds. Paper 64-588, International Council of the Aeronautical Sciences, Aug. 1964.
10. Laudeman, E.: Analysis of Supersonic Transport Takeoff Characteristics. Rep. AD-SST-014, Convair-San Diego, Sept. 5, 1961.
11. Urlich, W. F. W.: The Landing Flare of a Slender-Winged Supersonic Transport Aircraft. TN Aero.-2961, Royal Aircraft Establishment, May 1964.
12. Greatrex, F. B.: Take-Off and Landing of the Supersonic Transport - Noise Problems. Aircraft Engineering, vol. 35, no. 8, Aug. 1963, pp. 221-224.
13. Hubbard, Harvey H.; Cawthorn, Jimmy M.; and Copeland, W. Latham: Factors Relating to the Airport-Community Noise Problem. Conference on Aircraft Operating Problems, NASA SP-83, 1965, pp. 73-81.

14. Fischel, Jack; Butchart, Stanley P.; Robinson, Glenn H.; and Tremant, Robert A.: Flight Studies of Problems Pertinent to Low-Speed Operation of Jet Transports. Paper presented at NASA Conference on Some Problems Related to Aircraft Operation (Langley Field, Va.), Nov. 1958.
15. Magruder, W. M.; and McDonald, J. F.: Operating Techniques and Maintenance Practices for the Lockheed SST. Paper 660295, SAE, April 1966.
16. Anon.: Federal Aviation Regulations, Part 25 - Airworthiness Standards: Transport Category Airplanes. Federal Aviation Agency, Feb. 1, 1965.
17. Jameson, D. M.; and Chaplin, J. C.: Performance Safety Requirements for Civil Supersonic Transports. Paper 674 A, SAE and ASNE, April 1963.
18. Pinsker, W. J. G.: Some Observations on the Dynamics of Large Slender Aircraft. Paper presented at the AGARD Flight Mechanics Panel Stability and Control Session (Cambridge, England), Sept. 1966.
19. Bull, Gifford: Longitudinal Dynamics - A Critical Piloting Problem in Landing the Supersonic Transport. Paper presented at 6th Annual Symposium and Banquet, The Society of Experimental Test Pilots, Sept. 1962, p. 42.
20. Chalk, Charles R.: Flight Evaluation of Various Short Period Dynamics at Four Drag Configurations for the Landing Approach Task. Rep. FDL-TDR-64-60, Cornell Aeronautical Lab., Oct. 1964.
21. Staff of Servomechanisms Section and Aerodynamics Section, Northrop Aircraft, Inc.: Dynamics of the Airframe. Bu Aer Rep. AE-61-4-II, Northrop Corp., Norair Division, Sept. 1952.
22. Koven, William; and Wasicko, Richard: Flying Quality Requirements for United States Navy and Air Force Aircraft. AGARD Rep. 336, April 1961.
23. Kemp, William B., Jr.; Lockwood, Vernard E.; and Phillips, W. Pelham: Ground Effects Related to Landing of Airplanes With Low-Aspect-Ratio Wings. NASA TN D-3583, 1966.
24. Magruder, W. M.: A Pilot's View of Certification Testing and Development of Operational Procedures for Jet Transports. Paper 348 D, SAE, 1961.

02U 001 27 51 3DS 00903  
AIR FORCE WEAPONS LABORATORY/AFWL/  
KIRTLAND AIR FORCE BASE, NEW MEXICO 87117

ATT MISS MADELINE F. CANOVA, CHIEF TECHNIC  
LIBRARY /WLIL/

POSTMASTER: If Undeliverable (Section 15/  
Postal Manual) Do Not Return

*"The aeronautical and space activities of the United States shall be conducted so as to contribute . . . to the expansion of human knowledge of phenomena in the atmosphere and space. The Administration shall provide for the widest practicable and appropriate dissemination of information concerning its activities and the results thereof."*

—NATIONAL AERONAUTICS AND SPACE ACT OF 1958

## NASA SCIENTIFIC AND TECHNICAL PUBLICATIONS

**TECHNICAL REPORTS:** Scientific and technical information considered important, complete, and a lasting contribution to existing knowledge.

**TECHNICAL NOTES:** Information less broad in scope but nevertheless of importance as a contribution to existing knowledge.

**TECHNICAL MEMORANDUMS:** Information receiving limited distribution because of preliminary data, security classification, or other reasons.

**CONTRACTOR REPORTS:** Scientific and technical information generated under a NASA contract or grant and considered an important contribution to existing knowledge.

**TECHNICAL TRANSLATIONS:** Information published in a foreign language considered to merit NASA distribution in English.

**SPECIAL PUBLICATIONS:** Information derived from or of value to NASA activities. Publications include conference proceedings, monographs, data compilations, handbooks, sourcebooks, and special bibliographies.

**TECHNOLOGY UTILIZATION PUBLICATIONS:** Information on technology used by NASA that may be of particular interest in commercial and other non-aerospace applications. Publications include Tech Briefs, Technology Utilization Reports and Notes, and Technology Surveys.

*Details on the availability of these publications may be obtained from:*

SCIENTIFIC AND TECHNICAL INFORMATION DIVISION  
NATIONAL AERONAUTICS AND SPACE ADMINISTRATION

Washington, D.C. 20546